Although omeprazole is an AhR activator, no experimental evidence about its carcinogenic activity and metabolic activation has been reported [20]. Omeprazole, when administered at the clinical level, does not cause toxicity through AhR activation [21]. The possibility that omeprazole aggravates the effect of precarcinogens through CYP1A1 induction, however, still remains.

In this study, we exposed human and mouse hepatoma cells to benzo[a]pyrene and omeprazole simultaneously to examine the synergistic effect of these chemicals. Unexpectedly, we found that cytotoxicity of benzo[a]pyrene is alleviated by omeprazole exposure. We demonstrate that CYP1A1 induction through AhR activation and inhibition of CYP1A1 activity are significant effects of omeprazole in benzo[a]pyrene-treated cells.

Materials and Methods

Cell culture. Mouse hepatoma Hepa-1c1c7 and human hepatoma HepG2 cells were obtained from American Type Culture Collection (Rockville, MD, USA). The cells were grown with Dulbecco's modified Eagle's medium (Invitrogen, Carlsbad, CA, USA) containing 10% foetal bovine serum and antibiotics (Invitrogen). Cell cultures were carried out under standard ambient conditions at 37° and 5% CO_2.

Chemicals. Omeprazole, ethoxy-resorufin, ellipticine and ketoconazole were purchased from Sigma (St. Louis, MO, USA). Benzo[a]pyrene was obtained from Wako Pure Chemical (Osaka, Japan). Neutral red was obtained from Nacalai Tesque (Kyoto, Japan). Benzo[a]pyrene was dissolved in acetone and other compounds were dissolved in dimethyl sulfoxide. All the compounds were added to cultured cells to obtain a solvent with a final concentration of 0.1%.

Neutral red uptake assay. Cells were incubated on 48-well tissue culture plates at a concentration of 0.5×10^4 cells in 200 µl per well. After benzo[a]pyrene exposure for 24 hr, the medium was replaced by fresh medium containing 50 µg/ml neutral red. After incubation for another hour, the medium was removed. The cells were carefully washed twice with phosphate-buffered saline (PBS), and the neutral red incorporated into the cells was extracted with 100 µl of ethanol containing 1% acetic acid. Neutral red absorbance value at a wavelength of 570 nm was measured with the Model 550 microplate reader (Bio-Rad, Hercules, CA, USA).

Real-time reverse transcription–polymerase chain reaction analysis. Cells plated in 6-well plates at 80% confluence were exposed to a combination of omeprazole and benzo[a]pyrene. After 8 hr of exposure, total RNA was isolated using Isogen (Nippon Gene, Tokyo, Japan) according to the manufacturer's instructions. An aliquot (2 µg) of total RNA was subjected to reverse transcription in a 40-µl reaction mixture containing 0.5 mM dNTP (dATP, dCTP, dGTP, and dTTP), 25 U reverse transcriptase (MultiScribe; Applied Biosystems, Foster City, CA, USA), 2.5 µM oligo (dT) primers, 1× reverse transcriptase buffer and 5.5 mM $MgCl_2$. The reaction mixture was incubated with stepwise increases in temperature at 25° for 10 min., 48° for 40 min., and 95° for 5 min.

For mouse and human CYP1A1 mRNA quantification, real-time polymerase chain reaction (PCR) was performed by using the LightCycler instrument (Roche, Manheim, Germany). A primer pair for the mouse CYP1A1 cDNA amplification was as follows: forward primer, 5′-TAAAACACGCCCGCTGTGAA-3′; reverse primer, 5′-AAGTAGGAGGCAGGCACAATGTC-3′. A primer pair for the human CYP1A1 cDNA amplification was as follows: forward primer, 5′-CATAGACACTGATCTGGCTGCAG-3′; reverse primer, 5′-GGGAAGGCTCCATCAGCATC-3′. The human and mouse CYP1A1 cDNA fragments were amplified by Taq DNA polymerase (Gene Taq; Nippon Gene) with the primers described above and then inserted into a pGEM-T easy vector individually. The molecular weight of each plasmid DNA was calculated and its stock solution was diluted from 2×10^7 to 2×10^3 copies/µl for generating the calibrator DNA. An aliquot of the cDNA (2 µl) or calibrator plasmid DNA was amplified along with a master mixture (Fast-Start SYBR Green I kit; Roche) containing the CYP1A1-specific primers described above at a final volume of 20 µl. The reaction mixture was amplified under the following cycle condition: an initial incubation of 95° for 15 min. followed by 40 cycles of 95° for 15 sec., 60° for 20 sec., and 72° for 10 sec. The fluorescent products were detected at the end of the 72° extension period. To confirm amplification specificity, the PCR products were subjected to a melting curve analysis. The calibration curve was generated by threshold cycles of calibrators with a known copy number. The starting quantity of CYP1A1 mRNA in the samples was determined from correlation of their threshold cycles to the calibration curve.

Western blot analysis. CYP1A1 protein was detected by immunoblot analysis using polyclonal antibody against human CYP1A1 (Daiichi Pure Chemicals, Tokyo, Japan). Cells were plated on a 6-well plate at a density of 4×10^4 cells per well. After 16 hr of benzo[a]pyrene (1.25 µg/ml) and/or omeprazole (50 and 100 µM) treatment, the cells were lysed with 500 µl of sodium dodecyl sulfate (SDS) sample buffer (62.5 mM Tris-HCl, pH 7.4, 2% SDS). The total cell lysates were sonicated on ice in a 1.5-ml microcentrifuge tube for 30 sec. and then centrifuged at 20,000 ×g for 10 min. at 4°. Protein concentration of each sample was determined by the Bradford dye-binding method (Protein assay; Bio-Rad). An aliquot of 20 µg of protein was denatured by adding 2-mercaptoethanol (final concentration 5%) and heated at 95° for 3 min. The samples were allowed to cool to room temperature, and denatured samples were separated on a denaturing polyacrylamide gradient-buffered gel (ExelGel SDS Homogenous 7.5; GE Healthcare Biosciences, Tokyo, Japan) using Multiphor II Electrophoresis Unit (GE Healthcare Biosciences). The proteins were then electrophoretically transferred to nitrocellulose membranes. The membranes were soaked with blocking buffer (Block Ace; Daiichi Pure Chemicals) and probed with anti-rat CYP1A1 goat serum (Daiichi Pure Chemicals) or rabbit anti-actin polyclonal antibody (Sigma). The membranes were washed thoroughly with PBS containing 0.05% Tween-20. Antigen–antibody complexes were detected using horseradish peroxidase-conjugated anti-goat IgG (Chemicon International, Temecula, CA, USA) or anti-rabbit IgG (GE Healthcare Bioscience) with a chemiluminescence detection system (GE Healthcare Bioscience). For quantitative analysis, X-ray film was photographed by Printgraph (AE-6905H Image Saver; ATTO Bioinstrument, Tokyo, Japan), and the individual bands were quantified using a CS Analyser 2.0 system (ATTO Bioinstrument).

7-Ethoxy-resorufin-O-deethylase assay. 7-Ethoxy-resorufin-O-deethylase (EROD) assays were performed on intact living Hepa-1c1c7 cells as reported previously [22]. Cells were plated in 12-well plates (3×10^6 cells/well), allowed to grow to confluence, and treated with 1 µg/ml benzo[a]pyrene concomitantly with or without omeprazole (50 and 100 µM) in 500 µl of growth medium for 12 hr. Then, the medium was removed and the cells were washed with PBS. The assay was carried out by adding ethoxy-resorufin (final concentration, 5 mM) to the phenol red-free medium in the presence of newly added omeprazole with the same concentration of pre-treatment. The fluorescence of resorufin generated from the conversion of 7-ethoxy-resorufin by CYP1A1 was measured every 20 min. for 60 min. using a Labsystems Fluoroskan II fluorescence microplate reader (GMI Inc., Ramsey, MN, USA) with excitation at 544 nm and emission at 590 nm. A standard curve was constructed using resorufin. The EROD activity was expressed by quantification of resorufin as femtomole/10^{-5} cell/min.

Measurement of inhibition of human CYP activity by omeprazole. CYP activity was determined using P450-Glo CYP1A1 Assays, P450-Glo CYP3A4 Assays and P450-Glo CYP1A2 Assays (Promega, Madison, WI, USA) according to the manufacturer's instructions. The Sf9 cell microsomes containing recombinant human CYPs were purchased from Daiichi Pure Chemicals (Tokyo, Japan). An aliquot (0.5 µl) of microsomes was mixed with 100 mM KPO_4 buffer (25 µl) containing 120 µM of luciferin-6′-chloroethyl ether (CYP1A1), 120 µM of luciferin-6′-benzyl ether (CYP3A4) or 400 µM of luciferin-6′-methyl ether (CYP1A2). A 12.5-µl solution of omeprazole (0–500 µM) was added to each reaction cocktail and the mixtures were then incubated at 37° for 10 min. After preincubation, 25 µl of a 2× NADPH regenerating system solution (2.6 mM $NADP^+$, 6.6 mM glucose-6-phoshate, 0.4 unit/ml glucose-6-phoshate dehydrogenase and 6.6 mM $MgCl_2$) was added and the mixtures were incubated at 37° for 30 min. Luciferin converted from specific substrates by CYPs was detected by adding the Luciferin Detection Reagent included in the assay kit, and luminescence was determined in the Wallac Arvo SX Multi-Label counter (PerkinElmer, Boston, MA, USA). In order to determine IC_{50} values, activities were calculated with different omeprazole concentrations. Control activity was taken as 100% and the inhibitor concentrations causing 50% inhibition were determined from the graphs. In order to determine K_i constants with or without inhibitor, the assay was carried out with the various substrate (luciferin-6′-chloroethyl ether) concentrations (0.06, 0.12, 0.18, 0.24 and 0.30 mM), and the CYP1A1 activity was detected every 10 min. Lineweaver–Burk plots were drawn using 1/V versus 1/[S] values, and K_i constants were calculated from these graphs.

Results

Effect of omeprazole on benzo[a]pyrene toxicity in mouse and human hepatoma cells.

Omeprazole prevented the benzo[a]pyrene cytotoxicity in Hepa-1c1c7 and HepG2 cells in a dose-dependent manner as shown in fig. 1. This protection was more effective in Hepa-1c1c7 cells (fig. 1B and D) compared to HepG2 cells (fig. 1A and C). By the simultaneous exposure of omeprazole with variable doses of benzo[a]pyrene to Hepa-1c1c7 cells, cell death caused by the low-dose benzo[a]pyrene exposure (up to 0.75 mg/ml) was completely blocked by 100 µM omeprazole as shown in fig. 1B. Similar results were obtained in the experiment in which omeprazole was pre-treated 24 hr before benzo[a]pyrene exposure (data not shown).

Effect of omeprazole on benzo[a]pyrene-mediated CYP1A1 mRNA induction.

CYP1A1 mRNA was induced (18-fold compared to control) by the 50 µM omeprazole exposure alone in HepG2 cells (fig. 2A), while it was not induced in Hepa-1c1c7 cells (fig. 2C). Neither 10 µM nor 25 µM omeprazole exposure could induce CYP1A1 mRNA in HepG2 cells (data not shown). By exposure of benzo[a]pyrene (1 µg/ml), about 30-fold induction of CYP1A1 mRNA was obtained in Hepa-1c1c7 cells, and the induction was enhanced by dose-dependent addition of omeprazole (fig. 2D). In HepG2 cells, more than 200-fold induction of CYP1A1 mRNA was obtained by benzo[a]pyrene (1 µg/ml), and the induction was enhanced by adding 50 µM omeprazole but barely enhanced by adding 100 µM omeprazole (fig. 2B). These results suggest that the reduction of benzo[a]pyrene cytotoxicity by omeprazole observed in fig. 1 is not due to the inhibition of the transcriptional activation of CYP1A1.

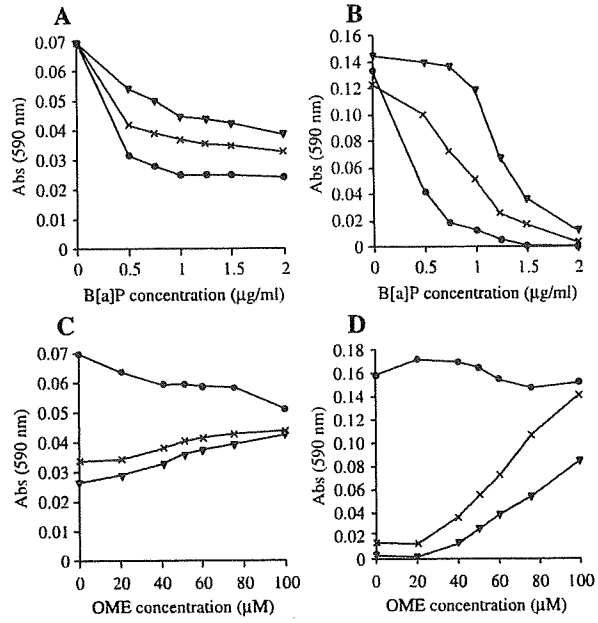

Fig. 1. Synergistic effects of omeprazole (OME) on benzo[a]pyrene (B[a]P)-induced cytotoxicity measured by neutral red uptake assay. HepG2 (A, C) and Hepa-1c1c7 cells (B, D) were plated in 48-well tissue culture plates. (A, B) Cells were exposed to a mixture of fixed concentration of OME (●, DMSO control; ×, 50 µM; ▼, 100 µM) with various concentrations (0–2 µg/ml)of B[a]P. (C, D) Cells were exposed to a mixture of fixed concentration of B[a]P (●, DMSO control; ×, 1 µg/ml; ▼, 1.5 µg/ml) with various concentrations of OME (0–100 µM). After 24 hr of exposure, the cell number was determined by neutral red uptake assay. The data points represent the mean of duplicate determinations. DMSO, dimethyl sulfoxide.

Effect of omeprazole on CYP1A1 protein induction.

The CYP1A1 protein levels detected by Western blot analysis and quantitative analysis are shown in fig. 3. CYP1A1 protein could not be detected in Hepa-1c1c7 cells by dimethyl sulfoxide (control) or omeprazole treatment (fig. 3B). Weak bands were detected in HepG2 cells treated with 100 µM omeprazole (fig. 3A). In both cell lines, the CYP1A1 protein levels were significantly induced by benzo[a]pyrene exposure and were not altered by the addition of omeprazole. These results suggest that the alleviation of benzo[a]pyrene cytotoxicity by omeprazole observed in fig. 1 is not due to inhibition of CYP1A1 translation or the effects on the turnover of the CYP1A1 protein.

Effect of omeprazole on EROD activity.

The effect of omeprazole on the CYP1A1 activity was evaluated by the EROD assay (fig. 4). The EROD activity was significantly increased by benzo[a]pyrene exposure in both cell lines (fig. 4A versus B; fig. 4C versus D). The basal EROD activity was inhibited by the treatment with omeprazole alone in Hepa-1c1c cells (fig. 4C), but not in HepG2

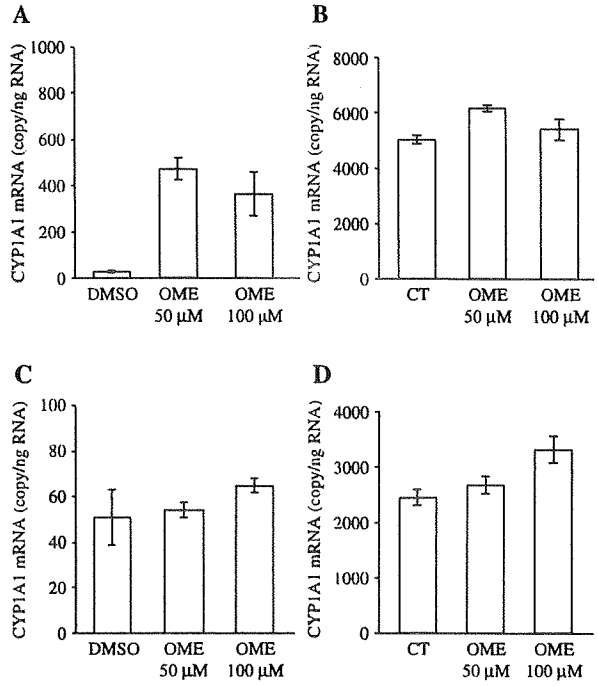

Fig. 2. Effects of omeprazole (OME) on CYP1A1 mRNA expression induced by benzo[a]pyrene (B[a]P). HepG2 cells (A, B) and Hepa-1c1c7 cells (C, D) were plated in 6-well tissue culture plates and exposed to OME (DMSO, 50 μM, 100 μM) concomitantly with (B, D: closed bar) or without 1 μg/ml of B[a]P (A, C: open bar). 'CT' represents control without OME but in the presence of B[a]P. After 8 hr of exposure, total RNA was isolated and human and mouse CYP1A1 mRNA were detected by real-time PCR. Data represent the value of CYP1A1 mRNA copy number in 1 ng total RNA. The mean of three independent experiments with S.D. is illustrated. DMSO, dimethyl sulfoxide.

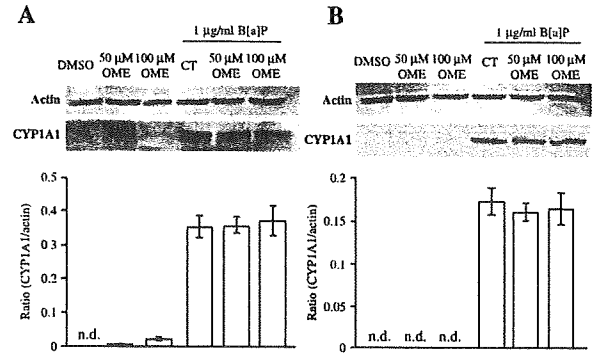

Fig. 3. Effects of omeprazole (OME) on CYP1A1 protein level induced by benzo[a]pyrene (B[a]P). HepG2 (A) or Hepa-1c1c7 cells (B) were plated in 6-well tissue culture plates and exposed to OME (DMSO, 50 μM, 100 μM) concomitantly with or without 1 μg/ml of B[a]P. 'CT' represents control without OME but in the presence of B[a]P. After 16 hr of exposure, cells were lysed with SDS sample buffer. The total cell lysates (20 μg protein) were analysed by Western blot for detecting CYP1A1 (lower panel) and actin (upper panel: internal control). The photographs shown are representatives of three independent experiments. The intensity of each band was quantified and the CYP1A1 protein level was normalized to the actin. Each column indicates the mean ± S.D. of the ratio of CYP1A1 protein to actin protein from three independent experiments. DMSO, dimethyl sulfoxide; n.d., not detected.

cells (fig. 4A). Omeprazole decreased the benzo[a]pyrene-induced EROD activity in both Hepa-1c1c7 and HepG2 cells in a similar fashion (fig. 4B and D). The inhibition of the EROD activity was stronger in Hepa-1c1c7 cells compared to HepG2 cells. As the EROD activity reflects CYP1A1 and CYP1A2 activities [23], these results suggest that omeprazole alleviates benzo[a]pyrene cytotoxicity by the inhibition of one or both of these CYPs.

Determination of CYP species responsible for the protection of benzo[a]pyrene cytotoxicity.

Benzo[a]pyrene induces not only CYP1A1 but also CYP3A4 and CYP1A2, and these CYPs also metabolize and activate benzo[a]pyrene. It is also known that omeprazole has inhibitory activity of CYP3A4. Therefore, we examined the effects of ellipticine (CYP1A1/1A2 inhibitor) and ketoconazole (CYP3A4 inhibitor) on the cytotoxicity of the benzo[a]pyrene exposure to clarify which CYP dominantly contributes to cytotoxicity in Hepa-1c1c7 cells. As shown in fig. 5, ellipticine protected cytotoxicity (fig. 5A), while ketoconazole did not, at least in the tested doses (fig. 5B). The experiment could not be carried out with higher concentrations of the inhibitors because of their own cytotoxicity (data not shown). These results suggest that CYP1A1 and CYP1A2 play a central role in the cytotoxicity induced by benzo[a]pyrene exposure.

Inhibition of recombinant human CYP activity by omeprazole.

The inhibition of CYP enzyme activity by omeprazole was measured with a specific substrate (fig. 6). CYP1A1 and CYP3A4 were inhibited by omeprazole in a dose-dependent manner, and IC_{50} values for the CYPs were 5.2 and 5.3 μM (fig. 6A and C, respectively). In contrast, omeprazole showed less inhibitory activity to CYP1A2 (IC_{50} > 100 μM) compared to CYP1A1 and CYP3A4 (fig. 6B). From the kinetic analysis shown in fig. 7, omeprazole was determined to be a competitive-type CYP1A1 inhibitor, because $1/V_{max}$ values, represented as the y-intercept, were almost the same with or without omeprazole (0.19 and 0.17) (fig. 7B). The K_i value of omeprazole against CYP1A1 activity was 3.21 μM and the K_m value of this enzyme was 50.1 μM.

Discussion

In the present study, to examine the possibility that omeprazole may aggravate the effect of environmental carcinogens through CYP1A1 induction, we exposed benzo[a]pyrene and omeprazole simultaneously to human and mouse hepatoma cells. Omeprazole-induced CYP1A1 induction has been reported to be species-specific, and it induces CYP1A1 through AhR activation in human cells, but not in mouse cells and tissues [12]. Therefore, it is expected that it does not affect benzo[a]pyrene cytotoxicity in mouse Hepa-1c1c7 cells, because the expression of CYP1A1 mRNA was barely

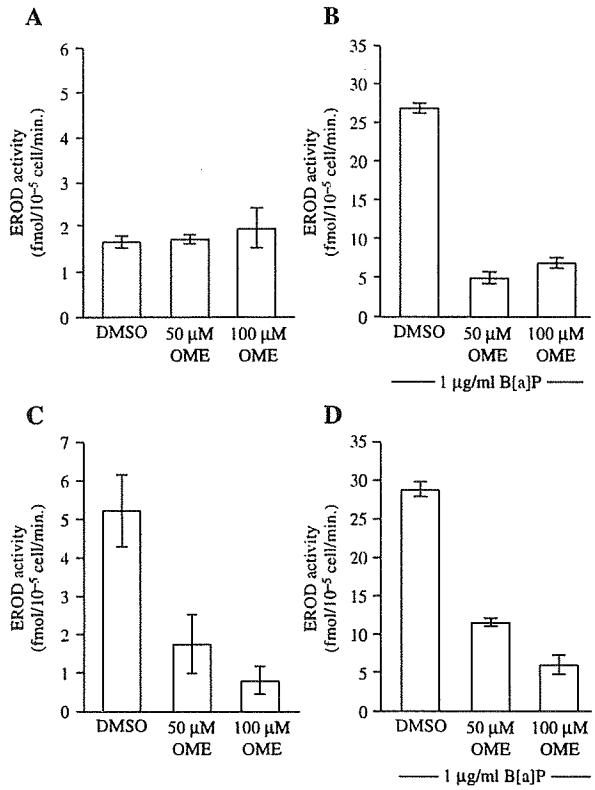

Fig. 4. Effects of omeprazole (OME) on EROD activity induced by benzo[a]pyrene (B[a]P). HepG2 (A, B) or Hepa-1c1c7 cells (C, D) were treated with OME (DMSO, 50, 100 μM) concomitantly with (B, D) or without (A, C) 1 μg/ml B[a]P for 12 hr. EROD activity was determined by adding 5 mM ethoxy-resorufin to the medium. The generated resorufin was measured after 60 min. of incubation by fluorescence plate reader with excitation at 544 nm and emission at 590 nm. Results represent the average of three independent experiments (mean ± S.D.). Note that the scales of the *x*-axis are different. DMSO, dimethyl sulfoxide.

induced (fig. 2C). Omeprazole induced CYP1A1 mRNA only in human HepG2 cells (fig. 2A). Contrary to expectation, omeprazole reduced benzo[a]pyrene cytotoxicity in both mouse and human cells in a similar fashion (fig. 1). These results suggest that the CYP1A1 induction by omeprazole could be irrelevant to the aggravation of benzo[a]pyrene cytotoxicity.

The cytotoxicity of benzo[a]pyrene requires metabolic activation by specific CYPs, because it is not reactive *per se*. If benzo[a]pyrene metabolites such as benzo[a]pyrene-7,8-dihydrodiol-9,10-epoxide were produced by CYPs, they form DNA adducts and represent cytotoxicity. In addition, reactive oxidant species generated as a by-product of CYP-mediated metabolic processes may be also involved in the toxicity. Several CYP species involved in benzo[a]pyrene metabolism have been reported, but which CYP species mainly mediates benzo[a]pyrene cytotoxicity is still controversial [17,23,24]. CYP1A1/2, 1B1, 3A4, 2C8 and 2C9/10 are considered to be the candidates for benzo[a]pyrene metabolism. A cell strain derived from Hepa-1c1c7 cells lacking AhR

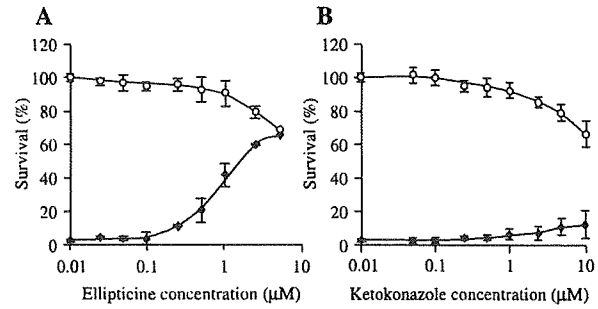

Fig. 5. Protective effects of CYP inhibitors on benzo[a]pyrene (B[a]P)-induced cytotoxicity in Hepa-1c1c7. (A) Cells were plated in a 48-well tissue culture plate and exposed to 0.01–3 μM ellipticine concomitantly with (◆) or without (○) 1 μg/ml of B[a]P. (B) Cells were exposed to 0.01–3 μM ketoconazole concomitantly with (◆) or without (○) 1 μg/ml B[a]P. After 24 hr of exposure, cell number was determined by neutral red uptake assay, and survival ratio was calculated by using absorbance of solvent control as 100%. Results represent the average of values from triplicate determinations (mean ± S.D.).

expression proved to be benzo[a]pyrene-resistant [19], which suggests that the manifestation of benzo[a]pyrene cytotoxicity requires the AhR-mediated induction of particular CYPs, CYP1A1, CYP1A2, CYP1B1 and CYP3A4. In HepG2 cells, CYP1A1 was induced by omeprazole alone, but the high level of CYP1A1 induced by benzo[a]pyrene was not affected by the simultaneous omeprazole treatment (figs 2A,B and 3). These results suggest that activation of the AhR pathway by omeprazole could not be involved in the aggravation of benzo[a]pyrene cytotoxicity in HepG2 cells.

The EROD assay clearly showed that omeprazole inhibits the EROD activity (i.e. CYP1A1/1A2 activity) [25], in intact Hepa-1c1c7 cells (fig. 4C). The experiment using recombinant human CYPs revealed that omeprazole has potent inhibitory activity against CYP1A1 and CYP3A4, but not against CYP1A2 (fig. 6). The CYP1B1 activity was not measured, because this enzyme is not expressed in HepG2 cells [8,26]. These results suggest that omeprazole alleviated benzo[a]pyrene cytotoxicity by directly inhibiting the CYP1A1 and/or CYP3A4 enzymatic activity.

We examined the effects of ellipticine, a CYP1A1 inhibitor [27], and ketoconazole, a CYP3A4 inhibitor [28], on benzo[a]pyrene cytotoxicity to confirm which CYP dominantly contributes to the toxicity. Ketoconazole reduced benzo[a]pyrene cytotoxicity in Hepa-1c1c7 cells only at high doses (>10 μM) (fig. 5). However, it has been reported that ketoconazole inhibits CYP3A4 at much lower doses (<1 μM). For example, ketoconazole inhibits testosterone 11β-hydroxylation with IC_{50} value at 0.03 μM, and erythromycin *N*-demethylation with K_i value at 0.7 μM [29,30]. These results show that CYP3A4 should not contribute dominantly to benzo[a]pyrene cytotoxicity. In contrast, the CYP1A1 inhibitor ellipticine completely blocked benzo[a]pyrene cytotoxicity (fig. 5). The kinetic analysis revealed that omeprazole is a potent inhibitor of CYP1A1, because the affinity of omeprazole to the enzyme is stronger than that to

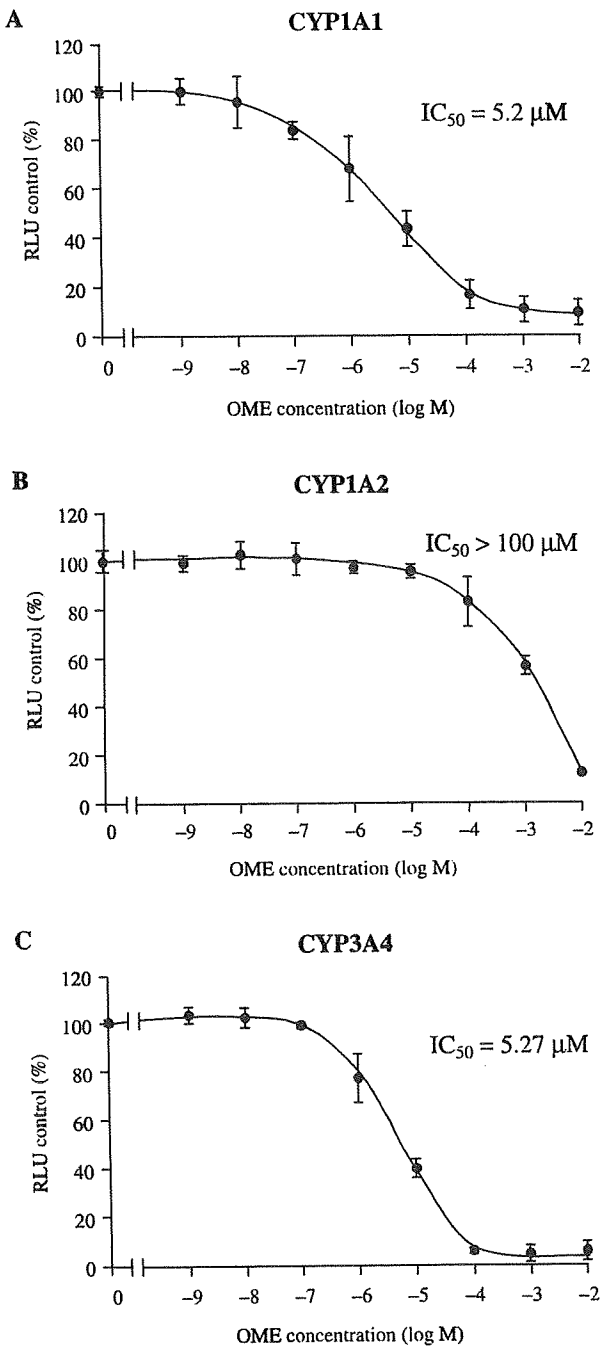

Fig. 6. Inhibition of recombinant human CYP activity by omeprazole (OME). CYP1A1 (A), 1A2 (B) and 3A4 (C) activity was determined using P450-Glo Assays and Sf9 cell microsomes containing recombinant human CYPs. Particular substrates and microsomes for each CYP were incubated at 37° for 30 min. with various concentrations of OME. The figure represents mean ± S.D. of triplicate determinations. RLU, relative light unit.

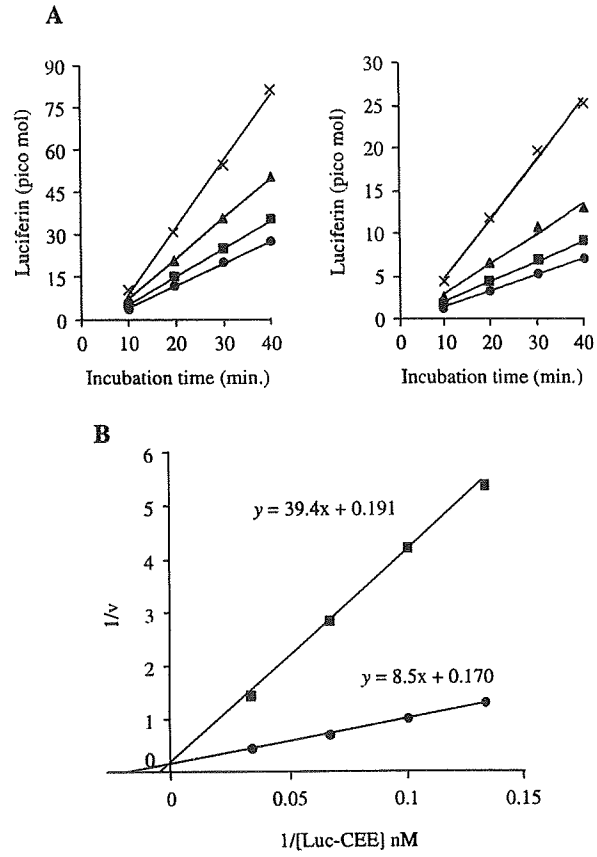

Fig. 7. Kinetic analysis of inhibition by omeprazole (OME) on human CYP1A1 activity. (A) CYP1A1 activity was determined using P450-Glo Assays and recombinant human CYP1A1 with various concentration of substrate in the absence (left) or presence (right) of OME. Assays were conducted in the presence of 10 μM OME and either 1 μM (●), 2.5 μM (■), 5 μM (▲) or 10 μM (×) of luciferin-6'-chloroethyl ether (Luc-CEE), and generated luciferin was measured every 10 min. for 40 min. Data shown are the mean of duplicate determinations from a single experiment. (B) Lineweaver–Burk plots of the CYP1A1 activity in the presence (●) or absence of 10 μM OME (■).

the substrate, that is, the K_i value (3.21 μM) is smaller than the K_m value (50.1 μM) (fig. 7). These results ensure that CYP1A1 dominantly contributes to benzo[a]pyrene cytotoxicity. We have determined the inhibition effect of omeprazole on CYP1A1 enzyme by using recombinant human CYP1A1. We expect mouse CYP1A1 also to be inhibited by omeprazole, because similar results of EROD activity inhibition were obtained in Hepa1c1c7 and HepG2 cells in our study (fig. 4).

Taken together, these findings indicate that omeprazole alleviates benzo[a]pyrene cytotoxicity by inhibiting the CYP1A1 activity in Hepa-1c1c7 and HepG2 cells. CYP1A1 is also a member of the CYP enzyme group that can be inhibited by omeprazole. The protection effect of omeprazole on the cytotoxicity of benzo[a]pyrene is more significant in Hepa1c1c7 than in HepG2 cells (fig. 1), although inhibition of EROD activity was comparable in both cell lines (fig. 4). Other causes, such as susceptibility to the reactive oxygen species, expression pattern of CYP species and the presence of omeprazole metabolites, may be involved in the protection effect, and these factors may be different between the two cell lines.

Figures 2 and 3 show that omeprazole concentration higher than 50 μM is required for the AhR-mediated CYP1A1 induction in HepG2 cells. This omeprazole concentration inhibits recombinant human CYP1A1 activity to less than 10% (fig. 6) and EROD activity in benzo[a]pyrene-treated HepG2 cells (fig. 4B). These results suggest that sufficiently high omeprazole concentrations to induce CYP1A1 inhibits CYP1A1 enzymatic activity, which in turn might indicate that omeprazole could not aggravate the effects of benzo[a]pyrene-type precarcinogens, which are chemicals metabolically activated by CYP1A1 through the AhR pathway.

Some phytochemicals, such as flavones and anthraquinone, have activities for both induction and inhibition of CYP1A1 [31–34]. Berberine, a plant isoquinoline alkaloid, has this 'biphasic effect' on CYP1A1 and has been used as a therapeutic agent like omeprazole [35]. To examine the aggravating effects of these chemicals on precarcinogens, it is necessary to carry out experiments similar to those of our present study.

Acknowledgements

This work was supported by the Environmental Technology Development Fund (Ministry of the Environment, Japan), Grant-in-aid for Scientific Research (Ministry of Education, Science, Sports and Culture, Japan) and Industrial Technology Research Grant Program in 2005 (New Energy and Industrial Technology Development Organization). We thank Mabel WL Chu for correcting English usage.

References

1 Lind T, Cederberg C, Ekenved G, Haglund U, Olbe L. Effect of omeprazole-a gastric proton pump inhibitor-on pentagastrin stimulated acid secretion in man. Gut 1983;**24**:270–6.
2 Ko J, Sukhova N, Thacker D, Chen P, Flockhart D. Evaluation of omeprazole and lansoprazole as inhibitors of cytochrome P450 isoforms. Drug Metab Dispos 1997;**25**:853–862.
3 Diaz D, Fabre I, Daujat M, Saint AB, Bories P, Michel H *et al.* Omeprazole is an aryl hydrocarbon-like inducer of human hepatic cytochrome P450. Gastroenterology 1990;**99**:737–47.
4 Curi-Pedrosa R, Daujat M, Pichard L, Ourlin JC, Clair P, Gervot L *et al.* Omeprazole and lansoprazole are mixed inducers of CYP1A and CYP3A in human hepatocytes in primary culture. J Pharmacol Exp Ther 1994;**269**:384–92.
5 Burbach KM, Poland A, Bradfield CA. Cloning of the Ah-receptor cDNA reveals a distinctive ligand-activated transcription factor. Proc Natl Acad Sci USA 1992;**89**:8185–9.
6 Denison MS, Fisher JM, Whitlock JP. Protein-DNA interactions at recognition sites for the dioxin-Ah receptor complex. J Biol Chem 1989;**264**:16478–82.
7 Reyes H, Reisz-Porszasz S, Hankinson O. Identification of the Ah receptor nuclear translocator protein (Arnt) as a component of the DNA binding form of the Ah receptor. Science 1992;**256**:1193–5.
8 Sutter TR, Tang YM, Hayes CL, Wo YY, Jabs EW, Li X *et al.* Complete cDNA sequence of a human dioxin-inducible mRNA identifies a new gene subfamily of cytochrome P450 that maps to chromosome 2. J Biol Chem 1994;**269**:13092–9.
9 Gu YZ, Hogenesch JB, Bradfield CA. The PAS superfamily: sensors of environmental and developmental signals. Annu Rev Pharmacol Toxicol 2000;**40**:519–61.
10 Daujat M, Peryt B, Lesca P, Fourtanier G, Domergue J, Maurel P. Omeprazole, an inducer of human CYP1A1 and 1A2, is not a ligand for the Ah receptor. Biochem Biophys Res Commun 1992;**188**:820–5.
11 Quattrochi LC, Tukey RH. Nuclear uptake of the Ah (dioxin) receptor in response to omeprazole: transcriptional activation of the human CYP1A1 gene. Mol Pharmacol 1993;**43**:504–8.
12 Kikuchi H, Hossain A, Sagami I, Ikawa S, Watanabe M. Different inducibility of cytochrome P-4501A1 mRNA of human and mouse by omeprazole in culture cells. Arch Biochem Biophys 1995;**316**:649–52.
13 Backlund M, Johansson I, Mkrtchian S, Ingelman-Sundberg M. Signal transduction-mediated activation of the aryl hydrocarbon receptor in rat hepatoma H4IIE cells. J Biol Chem. 1997;**272**:31755–63.
14 Backlund M, Ingelman-Sundberg M. Regulation of aryl hydrocarbon receptor signal transduction by protein tyrosine kinases. Cell Signal 2005;**17**:39–48.
15 Lemaire G, Delescluse C, Pralavorio M, Ledirac N, Lesca P, Rahmani R. The role of protein tyrosine kinases in CYP1A1 induction by omeprazole and thiabendazole in rat hepatocytes. Life Sci 2004;**74**:2265–78.
16 Okey AB, Dube AW, Vella LM. Binding of benzo(a)pyrene and dibenz(a,h)anthracene to the Ah receptor in mouse and rat hepatic cytosols. Cancer Res 1984;**44**:1426–32.
17 Gelboin HV. Benzo[a]pyrene metabolism, activation, and carcinogenesis: role and regulation of mixed-function oxidases and related enzymes. Physiol Rev 1980;**60**:1107–66.
18 Ko CB, Kim SJ, Park C, Kim BR, Shin CH, Choi S *et al.* Benzo(a)pyrene-induced apoptotic death of mouse hepatoma Hepa1c1c7 cells via activation of intrinsic caspase cascade and mitochondrial dysfunction. Toxicology 2004;**99**:35–46.
19 Zhang J, Watson AJ, Probst MR, Minehart E, Hankinson O. Basis for the loss of aryl hydrocarbon receptor gene expression in clones of a mouse hepatoma cell line. Mol Pharmacol 1996;**50**:1454–62.
20 Ekman L, Hansson E, Havu N, Carlsson E, Lundberg C. Toxicological studies on omeprazole. Scand J Gastroenterol Suppl 1985;**108**:53–69.
21 Salgueiro E, Rubio T, Hidalgo A, Manso G. Safety profile of proton pump inhibitors according to the spontaneous reports of suspected adverse reactions. Int J Clin Pharmacol Ther 2006;**44**:548–56.
22 Kennedy SW, Jones SP. Simultaneous measurement of cytochrome P4501A catalytic activity and total protein concentration with a fluorescence plate reader. Anal Biochem 1994;**222**:217–23.
23 Yun CH, Shimada T, Guengerich FP. Roles of human liver cytochrome P4502C and 3A enzymes in the 3-hydroxylation of benzo(a)pyrene. Cancer Res 1992;**52**:1868–74.
24 Nebert DW, Dalton TP, Okey AB, Gonzalez FJ. Role of aryl hydrocarbon receptor-mediated induction of the CYP1 enzymes in environmental toxicity and cancer. J Biol Chem 2004;**279**:23847–50.
25 Eugster HP, Probst M, Wurgler FE, Sengstag C. Caffeine, estradiol, and progesterone interact with human CYP1A1 and CYP1A2. Evidence from cDNA-directed expression in *Saccharomyces cerevisiae*. Drug Metab Dispos 1993;**21**:43–9.
26 Spink DC, Hayes CL, Young NR, Christou M, Sutter TR, Jefcoate CR *et al.* The effects of 2,3,7,8-tetrachlorodibenzo-p-dioxin on estrogen metabolism in MCF-7 breast cancer cells: evidence for induction of a novel 17 beta-estradiol 4-hydroxylase. J Steroid Biochem Mol Biol 1994;**51**:251–8.
27 Lesca P, Rafidinarivo E, Lecointe P, Mansuy D. A class of strong inhibitors of microsomal monooxygenases: the ellipticines. Chem Biol Interact 1979;**24**:189–97.
28 Sai Y, Dai R, Yang TJ, Krausz KW, Gonzalez FJ, Gelboin HV *et al.* Assessment of specificity of eight chemical inhibitors using

cDNA-expressed cytochromes P450. Xenobiotica 2000;**30**:327–43.

29 Choi MH, Skipper PL, Wishnok JS, Tannenbaum SR. Characterization of testosterone 11 beta-hydroxylation catalyzed by human liver microsomal cytochromes P450. Drug Metab Dispos 2005;**33**:714–8.

30 Rodrigues AD, Roberts EM, Mulford DJ, Yao Y, Ouellet D. Oxidative metabolism of clarithromycin in the presence of human liver microsomes. Major role for the cytochrome P4503A (CYP3A) subfamily. Drug Metab Dispos 1997;**25**:623–30

31 Sun M, Sakakibara H, Ashida H, Danno G, Kanazawa K. Cytochrome P4501A1-inhibitory action of antimutagenic anthraquinones in medicinal plants and the structure-activity relationship. Biosci Biotechnol Biochem 2000;**64**:1373–8.

32 Wang HW, Chen TL, Yang PC, Ueng TH. Induction of cytochromes P450 1A1 and 1B1 by emodin in human lung adenocarcinoma cell line CL5. Drug Metab Dispos 2001;**29**:1229–35.

33 Zhang S, Qin C, Safe SH. Flavonoids as aryl hydrocarbon receptor agonists/antagonists: effects of structure and cell context. Environ Health Perspect 2003;**111**:1877–82.

34 Chaudhary A, Willett KL. Inhibition of human cytochrome CYP 1 enzymes by flavonoids of St. John's wort. Toxicology 2006;**217**:194–205.

35 Vrzal R, Zdarilova A, Ulrichova J, Blaha L, Giesy JP, Dvorak Z. Activation of the aryl hydrocarbon receptor by berberine in HepG2 and H4IIE cells: Biphasic effect on CYP1A1. Biochem Pharmacol 2005;**70**:925–36.

JOURNAL OF APPLIED TOXICOLOGY
J. Appl. Toxicol. 2008
Published online in Wiley InterScience
(www.interscience.wiley.com) DOI: 10.1002/jat.1331

Differences in gene expression and benzo[a]pyrene-induced DNA adduct formation in the liver of three strains of female mice with identical *AhR*^{b2} genotype treated with 2,3,7,8-tetrachlorodibenzo-*p*-dioxin and/or benzo[a]pyrene

Qing Wu,[1] Junko S. Suzuki,[2] Hiroko Zaha,[2] Tien-Min Lin,[3] Richard E. Peterson,[3] Chiharu Tohyama[4] and Seiichiroh Ohsako[4,*]

[1] School of Public Health, Fudan University, 130 Dongan Road, Shanghai 200032, China
[2] Research Center for Environmental Risk, National Institute for Environmental Studies, 16-2 Onogawa, Tsukuba 305-8506, Japan
[3] School of Pharmacy and Molecular and Environmental Toxicology Center, University of Wisconsin, Madison, Wisconsin, USA
[4] Division of Environmental Health Sciences, Center for Disease Biology and Integrative Medicine, Graduate School of Medicine, The University of Tokyo, Hongo, Bunkyo-ku, Tokyo 113-0033, Japan

Received 19 June 2007; Revised 10 October 2007; Accepted 5 November 2007

ABSTRACT: To search for genes whose products modify aryl hydrocarbon receptor (AhR)-dependent toxicity caused by 2,3,7,8-tetrachlorodibenzo-p-dioxin (TCDD), gene expression profiles in the liver were surveyed using microarrays 24 h after the administration of TCDD to three strains of female mice, BALB/cAnN (BALB), C3H/HeN (C3H) and CBA/JN (CBA) all of identical AhR genotype. The BALB/cAnN strain had a more marked induction of a number of glutathione *S*-transferase (GST) sub-families, particularly the GSTmu gene family, compared with the other two strains. To assess the effects of GSTs induction to metabolize carcinogens, TCDD (40 μg kg^{-1}) was administered to BALB and CBA strains, followed 24 h later by an i.p. injection of low or high dose of benzo[a]pyrene (B[a]P, 50 or 200 mg kg^{-1}). The ^{32}P-postlabelling analysis showed that administration of TCDD alone failed to induce DNA adduct formation in both BALB and CBA strain mouse livers. The low dose of B[a]P alone produced DNA adduct in the liver of both strains to a similar extent. Treatment with TCDD 24 h before the low dose of B[a]P suppressed the formation of B[a]P-induced DNA-adduct more markedly in the BALB strain compared with the CBA strain. Taken together, these findings show that TCDD treatment causes strain-specific alterations in gene expression and B[a]P-induced DNA adduct formation in the liver of female mice of the same *AhR*^{b2} genotype. Furthermore, it suggests that TCDD-treated female mice of the BALB strain may have genes whose products modify the toxicity of B[a]P as evidenced by TCDD-induced alterations in B[a]P-DNA adduct formation. Copyright © 2008 John Wiley & Sons, Ltd.

Supplementary electronic material for this paper is available in Wiley Interscience at http://www.interscience.wiley.com/jpages/0260-437X/suppmat/jat.1331.html

KEY WORDS: aryl hydrocarbon receptor; benzo[a]pyrene; DNA-adduct; glutathione *S*-transferase; mouse, strain; 2,3,7,8-tetrachlorodibenzo-*p*-dioxin

Introduction

2,3,7,8-Tetrachlorodibenzo-*p*-dioxin (TCDD) is an environmental contaminant that is known to cause hepatotoxicity, teratogenicity and carcinogenicity (Schecter *et al.*, 2006). A characteristic feature in the toxicity of TCDD is exceptionally large differences in susceptibility among animal species or even strains belonging to the same species (Pohjanvirta and Tuomisto, 1994). Among inbred mouse strains, C57BL/6 is the most TCDD sensitive strain, while DBA/2 is less sensitive and requires a 10–20 times higher TCDD dose to manifest toxicity than the C57BL/6 strain (Chapman and Schiller, 1985). The C57BL/6 type of aryl hydrocarbon receptor (AhR) designated AhR^{b} has a 6-fold higher binding affinity than the DBA/2 type designated as AhR^{d} (Ema *et al.*, 1994). In addition, a C57BL/6 transgenic mouse strain in which the murine AhR was replaced with the human AhR showed less sensitivity to TCDD-induced teratogenicity than either the C57BL/6 or DBA/2 strains (Moriguchi *et al.*, 2003). A much greater difference (about 1000-fold) in susceptibility to the acute lethal effect of TCDD exists between two rat strains, Long-Evans (*Turku* AB; L-E) and Han/Wistar

* Correspondence to: Seiichiroh Ohsako, Division of Environmental Health Sciences, Center for Disease Biology and Integrative Medicine, Graduate School of Medicine, The University of Tokyo, Hongo, Bunkyo-ku, Tokyo 113-0033, Japan.
E-mail: ohsako@m.u-tokyo.ac.jp
Contract/grant sponsor: Environmental Technology Development Fund; Environmental Risk Office Fund of the Ministry of the Environment, Japan.

(*Kuopio*, H/W) (Unkila *et al.*, 1994). The H/W rat AhR has a *C*-terminal truncation of the transactivating domain compared with the L-E rat AhR (Pohjanvirta *et al.*, 1998). These interstrain differences in susceptibility to TCDD toxicity have been attributed to differences in AhR binding affinity and/or transcriptional activity in the various strains. Yet, a large difference in vulnerability to TCDD still exists that cannot be ascribed simply to polymorphisms of the *AhR* gene.

A quantitative trait locus analysis of an F2 intercross between C57BL/6 and DBA/2 strains showed that hepatic porphyria induced by pretreatment of iron compounds prior to TCDD administration depends on a gene locus that is independent from the *AhR* gene (Robinson *et al.*, 2002). In a Han/Wistar (*kupio*) strain that is very resistant to TCDD toxicity, a gene separate and distinct from the AhR may be responsible for the resistance to TCDD-induced lethality (Tuomisto *et al.*, 1999). Also TCDD treatment has been associated with placental disorders and fetal death in Holtzman rats, yet the same dose does not cause these effects in Sprague-Dawley rats even though both rat strains have an identical *AhR* genotype (Kawakami *et al.*, 2006). Furthermore, epididymal malformation by perinatal TCDD exposure was observed only in male Sprague-Dawley rats, not in Holtzman rats (Ohsako *et al.*, 2002). Together, these various findings suggest, in addition to the AhR, that other unknown gene products may exist that modulate TCDD toxicity in a strain- and species-dependent manner. Identification of these modifier genes is important for understanding the difference in susceptibility to TCDD toxicity among animal strains and species.

To test the hypothesis that there are genes whose products modify AhR dependent toxicities the study focused on benzo[a]pyrene (B[a]P)-induced DNA adduct formation in three mouse strains (BALB/c, CBA/J and C3H/He) that have an identical nucleotide sequence of the high affinity-type *AhR* gene, designated as AhR^{b2} (Thomas *et al.*, 2002). B[a]P is an extremely powerful carcinogen and its intermediate metabolite, benzo(a)pyrene 7,8-dihydrodiol-9,10-epioxide, is bioactivated by the classic TCDD inducible enzyme, cytochrome P4501A1 to form DNA adducts and act as an ultimate carcinogen (Sims *et al.*, 1974). The requirement of AhR to cause B[a]P induced skin carcinogenesis was demonstrated using AhR-null mice (Shimizu *et al.*, 2000). Unlike B[a]P, TCDD is not biotransformed to metabolites that directly react with DNA to form DNA adducts.

There were two overarching goals of the present study. The first was to determine the effect of TCDD treatment on gene expression in the liver of three strains of female mice having an identical *AhR* genotype (BALB, CBA and C3H). The second goal was to determine the effect of TCDD treatment on B[a]P-induced DNA-adduct formation in the liver of female mice from BALB and CBA that have the AhR^{b2} genotype in common.

Materials and Methods

Mice

Female BALB/cAnNCrj , CBA/JNCrj and C3H/HeNCrj strain mice were purchased from Charles River Japan, Inc. (Tokyo, Japan) and are referred to hereafter as BALB, C3H and CBA, respectively. The mice were provided food and water *ad libitum* and maintained in a controlled environment at a temperature of 24 ± 1 °C, a humidity of 45 ± 5% and a 12 h light/12 h dark cycle, and given free access to a solid diet (certified diet MF: Oriental Yeast Co., Tokyo, Japan) and distilled water. Animals were treated in a humane manner according to the National Institute for Environmental Studies' guidelines for animal experiments.

Exposure to TCDD and B[a]P

TCDD (>99.5% pure, 50 μg ml^{-1} in *n*-nonane) was purchased from Cambridge Isotope Laboratory (Andover, MA) and dissolved in corn oil (Sigma Aldrich, St Louis, MO) at serial concentrations of 0.1, 1.0 or 10.0 μg TCDD ml^{-1}. The *n*-nonane concentration was adjusted to 20% using *n*-nonane (Nacalai Tesque, Kyoto, Japan) and corn oil containing 20% *n*-nonane (Nacalai Tesque) was used as for the vehicle (control) treatment. B[a]P (Wako Pure Chemicals, Osaka, Japan) was dissolved in corn oil.

In an initial experiment, three 7-week-old, female mice were given a single oral dose of vehicle (control) or TCDD (40 μg kg^{-1}), euthanized by cervical dislocation 24 h later, and the livers removed. In a TCDD dose-response experiment, three females per dose were given a single oral dose of TCDD (0.4, 4.0 or 40 μg kg^{-1}) or an equivalent volume of vehicle (control). In both experiments, 24 h after exposure to vehicle or TCDD the mice were euthanized, the livers were quickly dissected from the carcasses and immediately placed into RNA*later* RNA Stabilization Reagent (Qiagen, Valencia, CA). For the TCDD-B[a]P exposure experiment, three females per group were given a single oral dose of TCDD (40 μg kg^{-1}), followed 24 h later by an intraperitoneal injection of B[a]P (50 or 200 mg kg^{-1}). Mice were killed by cervical dislocation 24 h after B[a]P administration, and livers were collected and kept at −80 °C for determination of DNA adducts.

Microarray Analysis

Total RNA was extracted from liver tissue samples from three female mice of each strain by using an RNeasy Mini Kit (Qiagen). Equivalent amounts of the RNA from each of the three livers per strain were mixed for the

DOI: 10.1002/jat

analysis for one array. cDNA synthesis, biotin-label cRNA synthesis and array analysis were performed according to the suppliers' protocols (Affymetrix, Santa Clara, CA). The Affymetrix GeneChip Mouse Expression Array 430A was used for the experiment. The GeneChip Operating Software (Affymetrix) was used to perform gene expression analysis. Gene expression levels in TCDD-exposed liver tissues from the three TCDD dose groups were compared with those of the vehicle control group, signal log two base ratios of >1 and <−1 were regarded as being significantly altered. Two independent experiments using a total of 18 arrays and 54 mice were performed for this array analysis. Pearson's correlation was used for hierarchical clustering with Gene Spring software (Agilent Technology, Tokyo, Japan).

Semiquantitative and Real-time RT-PCR

Semiquantitative and real-time RT-PCR were performed by our standard protocols (Kawakami *et al.*, 2006; Wu *et al.*, 2004) in order to amplify mouse CYP1A1, AhR, AhR nuclear translocator (ARNT), glutathione *S*-transferase mu 6 (GSTm6) and G3PDH mRNAs. Primer sequences used are summarized in Table 1. For semiquantitative RT-PCR, Hot Star Taq polymerase (Qiagen) was used. The reaction conditions were as follows: 1 cycle at 95 °C for 15 min, followed by 28 cycles of denaturation for 30 s at 94 °C, annealing for 30 s at 55 °C, and extension at 72 °C for 45 s. The PCR products were separated by electrophoresis on 2% agarose gels and photographed under a UV transilluminator. For the real-time RT-PCR, a QuantiTect SYBR Green PCR kit (Qiagen, Hilden, Germany) was used. The reaction conditions were as follows: 1 cycle at 95 °C for 15 min, followed by 35 cycles of denaturation for 15 s at 95 °C, annealing for 20 s at 56 °C, and extension at 72 °C for 20 s. After completion of the final cycle, a melting curve analysis was performed to monitor PCR product purity. Five serial dilutions ranging from 0.125 µl to 2 µl aliquots of the RT reaction products were used to construct a standard curve. The expression of the targeted gene transcript was calculated using linear extrapolation and normalized to that of the G3PDH gene. The expression ratios for the various genes were indicated relative to the mean expression ratio (adjusted to 1) in the control group.

Sequencing

The AhR-coding region (NM_013464) was amplified from liver cDNA using RT-PCR and LA Taq™ polymerase (TaKaRa Biomedicals, Otsu, Japan). The following four sets of primers were used for amplifying four DNA segments of the AhR coding region: forward-1, AGCCG GGAAG CCCTA GAGCA; reverse-1, AGACC AAGGC ATCTG CTGTG (621 bp amplicon); forward-2, AGTCC ACCCC TGCTG ACAGA AA; reverse-2, CGGAT GTGGG ATTCT GCACA (739 bp); forward-3, ACAAG AGGAT CGGGG TACCA; reverse-3, GATTT CGTCC GTTAT GTCGA (795 bp); forward-4, ACACT AGCAG GAAAG ACTGG; reverse-4, GAGCT CTCCC ATCGT ATAGG (1420 bp). Genomic DNA was isolated from mouse liver using a Wizard Genomic DNA purification kit (Promega, Madison, WI). The promoter region (−2237 to +340) of the GSTm6 gene (NT_039239.2) was amplified by PCR using the following primers: forward, GTGAC CCAGC TGTGA GAGAT; reverse, TGTCT CCCCT TCCAA CTCGT. The PCR products were directly sequenced using an Applied Biosystem 377-3100 Automated Sequencer, and the dideo-xynucleotide chain termination method was performed using a DYEnamic ET terminator cycle sequencing kit (Amersham Biosciences, Piscataway, NJ).

^{32}P-Postlabeling

B[a]P DNA adduct formation was determined by the ^{32}P-postlabeling method (Sato *et al.*, 2003; Uno *et al.*, 2004; Gupta *et al.*, 1982). In brief, DNA was extracted from liver samples by using a Wizard genome DNA isolation kit (Promega, Madison, WI). The DNA sample (8 µg) was digested with micrococcal endonuclease and spleen phosphodiesterase (Sigma-Aldrich) at 37 °C for 3 h, followed by a further digestion with nuclease P1 at 37 °C for 45 min. Tris-base was added to stop the reaction. The adduct nucleotides were labeled with [γ-^{32}P] ATP using T4 polynucleoside kinase at 37 °C for 30 min. Potato apyrase (Sigma-Aldrich) was added and the solution was cultured at 37 °C for 30 min to destroy excess ATP. After collecting a 1 µl aliquot of the ^{32}P-labeled solution for the determination of total nucleotides and ATP, the remaining ^{32}P labeled sample was applied to thin-layer

Table 1. Primers Used for RT-PCR

RT-PCR targets	Forward (5′ to 3′)	Reverse (5′ to 3′)	Product size	GenBank No.
CYP1A1	TGTTCACCCTACATAGAAACA	CAAGAGCTGATGCAGTAGTCTA	295bp	NM_009992
AhR	ATCCCACATCCGCATGATTAAG	GGGAGCCCAGTCTTTCCTGCTA	331bp	NM_013464
ARNT	CAGGCTACAGCCAAGACTCGTT	TGTGTCTGCTGAACATGCTGCT	284bp	NM_009709
GSTm6	TCGAATTCAGATGGGCATGCTT	GTACACAGGACTTGGAAGGAAGC	307bp	NM_008184
G3PDH	CACAGTCAAGGCCGAGAATG	TCTCGTGGTTCACACCCATC	382bp	M33599

DOI: 10.1002/jat

chromatography using a solvent system of 1 M sodium phosphate, pH 6.5 for developing direction 1; 3.5 M lithium formate, 8.5 M urea, pH 3.5 for direction 2; 0.8 M LiCl, 0.5 M Tris-HCl, 8.5 M urea, pH 8.0 for direction 3, 1.7 M sodium phosphate, pH 6.0 also for direction 3, on polyethylenimine (PEI) cellulose sheets (EM Science, Gibbstown, NJ). Autoradiography was used to detect DNA adducts, and their amounts were estimated as relative adduct level (RAL) = intensity of adduct nucleotides/(intensity of total nucleotides × dilution factor).

Statistical Analysis

StatView software for Windows version 5.0 (SAS Institute, Cary, NC) was used for statistical analyses. Means of gene expression levels and relative DNA-adduct levels for the TCDD and vehicle (control) treatment groups, respectively, were compared by one-way analysis of variance (ANOVA), followed by the Fisher PLSD test as a post-hoc test and Student's *t*-test. Significance was set at $P \leq 0.05$.

Results

TCDD-induced Alterations in Gene Expression in the Three Strains of Mice

According to the microarray analysis, the liver from TCDD-exposed, female BALB strain mice had 67 up-regulated and 71 down-regulated gene transcripts out of 22 690 gene transcripts, while fewer numbers of genes were altered in the liver of TCDD-exposed, female C3H and CBA strains of mice (See our website <http://www.nies.go.jp/health/drgdb/drgdb-top/TOP.htm> for DIOXIN RESPONSIVE GENE DATABASE, DRGdb-NIES). Direct sequence analyses demonstrated that the three mouse strains, BALB, C3H and CBA, had an identical nucleotide sequence in the entire open reading frame of *AhR* gene (results not shown), and a battery of AhR-dependent genes, such as CYP1A1, CYP1A2 and CYP1B1, were up-regulated by TCDD in all three strains. On the other hand, it was found that genes that were regulated by TCDD (40 μg kg^{-1}) in one strain were not necessarily regulated in the other two strains (Table 2). According

Table 2. Three strains of female mice (BALB, C3H and CBA) with identical *AhR*^{b2} genotype exhibit unique, strain-specific alterations in hepatic gene expression 24 h after exposure to a high dose of TCDD (40 μg kg^{-1})

UniGene ID	Gene title	Level[a]
BALB only		
Mm.10742	Cytochrome P450, family 4, subfamily a, polypeptide 10	2.10
Mm.31041	Glutathione *S*-transferase, mu 6	1.69
Mm.2935	RIKEN cDNA 4631408O11 gene	1.67
Mm.18064	Glucose-6-phosphatase, catalytic	1.60
Mm.4871	Tissue inhibitor of metalloproteinase 3	1.45
Mm.36742	ADAM-like, decysin 1	1.36
Mm.41116	Solute carrier family 25, member 30	1.36
Mm.6716	Histocompatibility 2, class II antigen A, beta 1	1.33
Mm.33653	Wingless-related MMTV integration site 2	1.23
Mm.23551	Ubiquitin-conjugating enzyme E2E 2 (UBC4/5 homolog, yeast)	1.16
Mm.2165	Serum amyloid P-component	−1.19
Mm.29094	Serine (or cysteine) proteinase inhibitor, clade A (alpha-1 antiproteinase, antitrypsin), member 10	−1.21
Mm.13787	Ceruloplasmin	−1.25
Mm.2774	Deiodinase, iodothyronine, type I	−1.54
Mm.200230	Adenosine A1 receptor	−1.91
Mm.69061	Guanine nucleotide binding protein, alpha transducing 1	−1.99
Mm.15675	Ephrin A1	−2.11
Mm.20286	Serine (or cysteine) proteinase inhibitor, clade A (alpha-1 antiproteinase, antitrypsin), member 12	−2.53
Mm.27334	Vanin 3	−2.98
Mm.31403	Tumor necrosis factor, alpha-induced protein 9	−3.34
C3H only		
Mm.29908	Dynein, cytoplasmic, light chain 1	1.26
Mm.30163	Ethanolamine kinase 1	1.09
Mm.6856	Pituitary tumor-transforming 1	−1.20
Mm.2131	Elastase 1, pancreatic	−1.26
Mm.28305	Hypothetical protein LOC223672	−1.32
Mm.41911	Cytochrome P450, family 46, subfamily a, polypeptide 1	−1.34
Mm.2580	Syndecan 1	−1.37
Mm.28685	Serine dehydratase	−1.42
Mm.22331	Monocyte to macrophage differentiation-associated 2	−1.86
CBA only		
Mm.25613	Immediate early response 3	2.21
Mm.195091	X-linked lymphocyte-regulated 3a	1.17
Mm.13020	Transcription factor 4	1.15
Mm.33353	Rho GTPase activating protein 6	−1.63

[a] Up- or down-regulation level was shown as the average Signal Log Ratio for comparisons (vehicle vs TCDD). Results were from two independent experiments.

DOI: 10.1002/jat

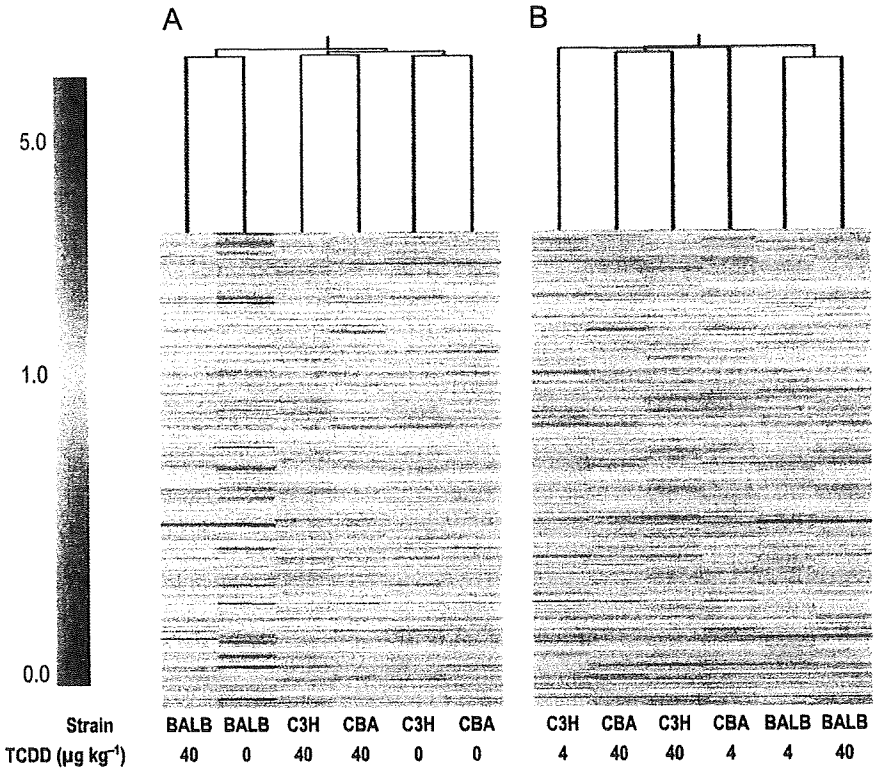

Figure 1. Hierarchical clustering analysis of microarray data. Hierarchical clustering analysis of the expression levels of the 22 690 probe sets contained on the microarrays for liver samples obtained from female BALB, C3H and CBA mice 24 h after treatment with either vehicle or 40 μg kg^{-1} TCDD. The signal intensity and the Trust were calculated and the clustering analyses were performed using GeneSpring software. The range of the signal intensity and the Trust, defined by the GeneSpring, are represented by colors, as shown by the color scale in the left bar. On the horizontal axis, the six samples were clustered based on a comparison of the overall pattern of gene expression in each sample. The length of the vertical lines connecting the different samples is proportional to the differences in liver expression patterns. (A) Comparison between vehicle and TCDD (40 μg kg^{-1}) treated liver samples. (B) Comparison between TCDD (4 μg kg^{-1}) and TCDD (40 μg kg^{-1}) treated liver samples. Note that the expression profiles of the C3H and CBA strains are similar, and BALB mice were in a different branch of the phylogenetic tree

to the gene clustering analysis, CBA and C3H strains presented similar expression-profile patterns, while BALB mice were allocated to a different branch of the phylogenetic tree (Fig. 1). These results suggest that global gene expression may be modulated differently by TCDD among strains with an identical AhR^{b2} genotype, due to different genetic backgrounds.

Induction of GST Gene Family by TCDD in BALB Mice

From the microarray data, the TCDD-exposed BALB strain had a higher expression level for five out of the six mu-class GST (GSTm) family genes than the TCDD-exposed C3H or CBA strains (Fig. 2). Other classes of GSTs, such as alpha-class GSTs (GSTa), theta-class GSTs (GSTt) and omega-class GSTs (GSTo), were also induced by TCDD at higher levels in BALB than in the other two mouse strains (Fig. 3). The GSTm6 mRNA expression levels were checked by real-time-RT-PCR and confirmed that they were dose-dependently increased by TCDD in the BALB strain, but not in the C3H and CBA strain mice (Fig. 4). There was no change in the expression levels of AhR and ARNT, while CYP1A1 mRNA was induced at a similar level in the livers of all three mouse strains (Fig. 4).

B[a]P-initiated DNA Adduct Formation upon TCDD Exposure

Since an elevated expression of GSTm was observed, possible differences were studied in susceptibility to the carcinogen B[a]P between the same three mouse strains that were pretreated with either vehicle (control) or TCDD. The level of B[a]P-induced DNA adduct formation in the liver of female mice of the BALB and CBA

DOI: 10.1002/jat

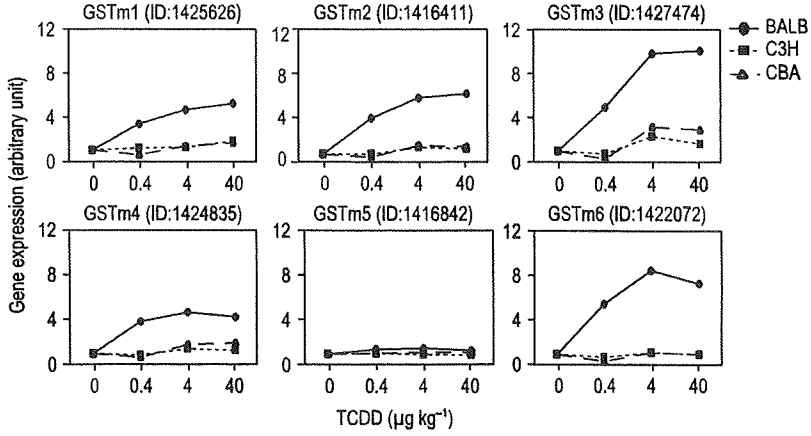

Figure 2. Induction of GSTm family genes in the liver of female BALB, C3H and CBA mice 24 h after exposure to vehicle or three graded doses of TCDD. Hepatic RNA specimens from three female mice were pooled as one array sample. The Affymetrix probe IDs of probe sets are shown in brackets to the right of the gene name. Horizontal and vertical axes represent TCDD dose (μg kg^{-1}) and fold-of-induction over vehicle-treated control, respectively. Note that five out of six GSTm genes, i.e. all except GSTm5, were up-regulated in the BALB strain

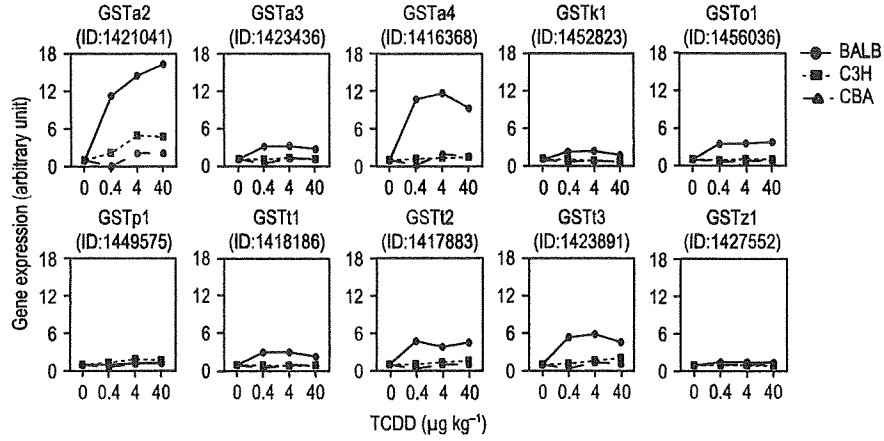

Figure 3. Induction of GST family genes, other than GSTm, in the liver of female mice of the BALB, C3H and CBA strains 24 h after exposure to vehicle (control, 0 μg kg^{-1}) or graded doses of TCDD (0.4, 4 or 40 μg kg^{-1}). Hepatic RNA specimens from three female mice of each strain were pooled as one array sample. The Affymetrix probe IDs of probe sets are shown in brackets to the right of each gene name. Horizontal and vertical axes represent TCDD dose (μg kg^{-1}) and fold-of-induction over the vehicle-treated control, respectively

strain was carried out using the ^{32}P-postlabeling method (Fig. 5). The B[a]P was administered 24 h after the treatment with vehicle (control) or TCDD.

Administration of TCDD alone failed to induce DNA adduct formation in both BALB and CBA strain mouse livers while B[a]P alone (50 mg kg^{-1}) produced DNA adduct in the liver of both strains to a similar extent (Fig. 5B). However, when B[a]P was administered 24 h after TCDD, the amount of DNA adducts formed were decreased to 20% and 36% of B[a]P treatment alone for both the BALB and CBA strains, respectively, and there was a significantly larger decrease for the BALB strain. On the other hand, when the B[a]P dose was increased to 200 mg kg^{-1} and given 24 h after TCDD, DNA adduct formation was increased approximately 2.3 and 2.0-fold over that observed in mice treated with the lower dose of B[a]P (50 mg kg^{-1}). This result was found for both BALB and CBA strains and there was no significant difference between the two strains (Fig. 5B).

Discussion

The susceptibility to xenochemicals is generally determined by various factors including absorption, distribution, metabolism and excretion. However, gene–environment interactions are an important research topic. It offers possible ways to define individual genetic risk profiles, which

DOI: 10.1002/jat

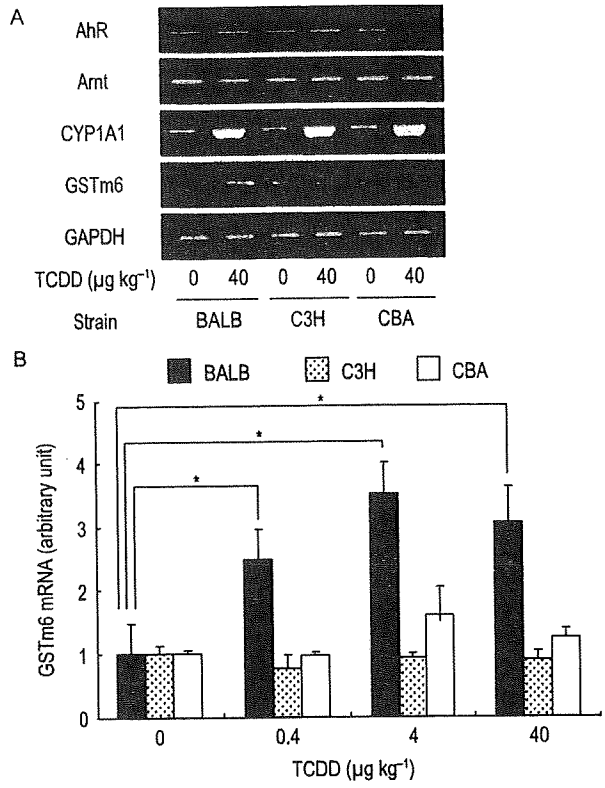

Figure 4. Gene expression levels of the CYP1A1, AhR, ARNT and GSTm6 in the liver of female mice from BALB, C3H and CBA strains having an identical AhR^{b2} genotype 24 h after exposure to vehicle (0 μg kg^{-1}) or TCDD (0.4, 4 or 40 μg kg^{-1}). (A) Image of electrophoretic gels of semi-quantitative RT-PCR. The hepatic mRNA levels for AhR, Arnt, and GAPDH was similar for vehicle and TCDD-exposed female mice of the BALB, C3H and CBA strains, respectively. CYP1A1 mRNA levels were induced by TCDD treatment in all three strains of female mice to a similar extent. On the other hand, the expression of GSTm6 mRNA in the liver of female mice was up-regulated only in the BALB strain. (B) Real-time PCR analysis of GSTm6 induction. Results are expressed as mean ± SE (n = 3). The expression level of GSTm6 was increased by TCDD in a dose-dependent manner only in the liver of female mice of the BALB strain. Asterisks in the bar graph showing GSTm6 mRNA abundance in the liver of female BALB strain mice indicate a statistically significant difference of the TCDD treatment groups (0.4, 4 and 40 μg kg^{-1}) from the vehicle-treated control (0 μg kg^{-1}) by ANOVA with a post-hoc analysis ($P < 0.05$)

may identify a sub-population of people at risk of developing certain diseases such as cancer, that may be associated with environmental exposure. Susceptibility to carcinogens such as TCDD and B[a]P might be influenced by ligand-binding affinity of the AhR. Activation of the AhR in the liver can result in the detoxification or activation of a parent xenobiotic by phase I enzymes such as cytochrome P450 1A1 and 2. A typical example of metabolic activation is the diol epoxide of B[a]P by CYP1A1 in human lung tissue, followed by the further detoxification by the phase II drug metabolizing process. In particular, the diol epoxide of B[a]P undergoes glutathione conjugation (Gelboin, 1980) and null mutation of GST-mu has been suspected to be linked to cancer risk. More specifically, 50% of Caucasians lack the GSTM1 gene, which is thought to be related an increased risk of lung cancer in smokers (Bartsch, 2000). Thus, gene and environment interactions such as these are important considerations in the health risk assessment of xenochemicals such as B[a]P.

To search for genes that might modulate AhR signaling, three strains of mice were used, BALB, C3H and CBA, that have in common an AhR^{b2} genotype, characterized by high AhR^{b2} binding affinity for TCDD. Cluster analysis revealed that the pattern of TCDD-induced alterations in hepatic gene expression in BALB mice was different from that of C3H and CBA mice, with unique sets of genes being regulated following high dose TCDD exposure (40 μg kg^{-1}) in each strain (Table 2). Accordingly the TCDD-induced hepatic gene expression profile of BALB mice was classified differentially from that of C3H and CBA mice. The unique gene expression changes in the liver of BALB versus C3H and CBA female mice may convey strain-specific effects of TCDD between these strains. However, the function of most of these genes are unknown. Therefore, the present study focused on glutathione-*S*-transferases (GSTs) to study possible modifying effects of the mouse strain on TCDD-induced phase II enzymes. GSTs comprise two distinct superfamilies, and the larger superfamily consists of cytosolic enzymes that are principally, but not exclusively, involved in biotransformation of toxic xenobiotics while the other family is composed of microsomal enzymes, primarily involved in arachidonic acid metabolism (Hayes and Pulford, 1995). The GSTmu-class belongs to the former superfamily. It has been reported that GSTmu (GSTm) and pi (GSTp) are efficient in the conjugation of intermediate metabolites of polycyclic aromatic hydrocarbons (PAHs), including B[a]P diol epoxide (Robertson *et al.*, 1986; Sundberg *et al.*, 1997). The present results showed that the induction of *GSTp1* gene was not markedly enhanced and was not different among the three mouse strains (Fig. 3). However, *GSTm* genes were more markedly induced by TCDD in the liver of female mice in the BALB strain than in the other two strains, C3H and CBA (Fig. 2), GSTm6 was up-regulated by TCDD (40 μg kg^{-1}) only in BALB strain but not in the other C3H and CBA strains (Table 2). Therefore, female BALB and CBA strain mice were administered, respectively, B[a]P 24 h after vehicle (control) or TCDD treatment to study the effect of TCDD on the induction of GSTm involved in the detoxification of B[a]P as well as on B[a]P induced DNA-adduct formation. Consistent

DOI: 10.1002/jat

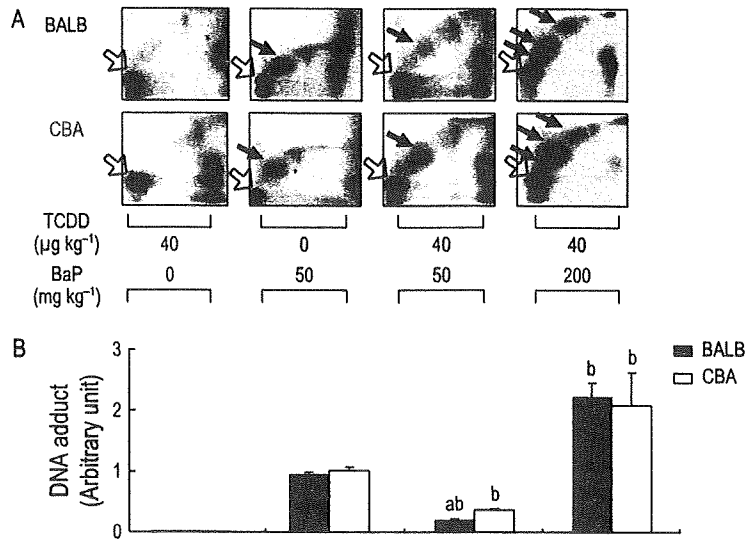

Figure 5. A representative result of DNA adduct formation. (A) Autoradiogram of B[a]P-DNA adducts detected by two-dimensional thin-layer chromatography using the ^{32}P-post labeling method. The open arrow indicates the point at which the ^{32}P-labeled DNA digested sample was applied. The solid arrow indicates the presence of B[a]P-DNA adducts. Liver samples from three mice were individually subjected to extraction of B[a]P-DNA adducts and applied to thin-layer chromatography. (B) Results are expressed as the mean ± SE (n = 3). Mean differences were analysed by Student's t-test. [a] BALB strain significantly different from the CBA strain for a specific TCDD and B[a]P treatment regimen ($P < 0.05$); [b] within the BALB strain or the CBA strain treated with both TCDD and B[a]P, respectively, the letter 'b' indicates a significant difference in DNA adduct formation ($P \leq 0.05$) compared with the TCDD only treatment group (40 μg kg^{-1} TCDD and 0 mg kg^{-1} B[a]P) and the B[a]P only treatment (0 μg kg^{-1} TCDD and 50 mg kg^{-1} B[a]P)

with GSTm-class genes being markedly induced by TCDD in BALB mice, it was found that the amount of B[a]P-DNA adduct formation was less in the liver of female mice of the BALB strain than of the CBA strain. B[a]P is a substrate for CYP1A1 and CYP1B1 and is metabolized by these phase I enzymes to form reactive intermediates that bind covalently to nucleic acids and proteins. B[a]P is detoxified by both phase I and phase II enzymes. B[a]P-DNA adduct formation depends on the balance between the activity of epoxidation and the activity of GST conjugation, which may be associated with CYP1A1 and CPY1B1 induction and GST family gene induction. In the present study, microarray data showed that CYP1A1 and CYP1B1 mRNA abundance were induced to similar levels in the liver of female BALB and CBA mice in two independent experiments. CYP1A1 induction was also checked by PCR. Therefore, the strain difference in formation of B[a]P-DNA adduct may be due to differential induction by TCDD of GST family genes. However, reduced formation of B[a]P-DNA adducts was only observed at the lowest dose of B[a]P tested (50 mg kg^{-1}) following TCDD exposure. At the higher B[a]P dose (200 mg kg^{-1}) following TCDD exposure there was not a significant strain difference in B[a]P-DNA adduct formation. The lack of a strain difference in response to TCDD treatment may have occurred because of the overwhelming high amount of B[a]P-induced DNA adduct formation in both mouse strains given the higher dose of B[a]P. The findings further suggest that the increased expression of GST family genes in the liver of female mice of the BALB strain may play a protecting role against AhR-dependent chemically induced carcinogenesis at low level in the liver of this strain.

Using liver samples from each of the BALB, CBA and C3H strains, genomic DNA of *GSTm6* was cloned, but no difference in sequence of the 5′-flanking sequence (-2255-bp) of *GSTm6* and no XRE motifs were found among the 5′-flanking sequence in the three strains (results not shown). It was also found that the XRE consensus sequence is not present in the 5′-flanking sequence of the promoter regions of the *GSTm1*, *GSTm2*, *GSTm3*, *GSTm4 and GSTm6* genes. While the mechanism of GSTm up-regulation by TCDD in BALB mice is unclear, it has been reported that phase I and phase II enzymes can be induced by TCDD and B[a]P through two distinct mechanisms: CYP1A1 is largely regulated by the XRE, whereas GST is largely regulated by the antioxidant response element (Prochaska and Talalay, 1988). The Keap1-Nrf2 system is known to regulate phase II drug-metabolizing enzymes by activating the antioxidant response element (Dinkova-Kostova *et al.*, 2002), and its activation by a chemoprotective agent, such as oltipraz, protects against B[a]P-induced stomach carcinogenesis (Ramos-Gomez *et al.*, 2001). Keap1-null mice have an increased level

DOI: 10.1002/jat

of GSTm gene expression, indicating that GSTm gene expression is regulated by the Keap1-Nrf2 system (Wakabayashi *et al.*, 2003). While the same system may play a role in enhancing GSTm expression only in BALB mice, the microarray results did not show a significant change of Nrf2 or Keap1 gene expression in the exposed group. Thus, possible involvement of the Nrf2/Keap1 system in the up-regulation of GSTm in TCDD-exposed female BALB mice, but not TCDD-exposed female C3H or CBA mice, will require further investigation. In the present study, administration of TCDD followed 24 h later by B[a]P (50 mg kg^{-1}) produced significantly fewer DNA adducts than after treatment with B[a]P alone. Although TCDD acts as a cancer promoter, Holcomb and Safe (1994) reported that TCDD inhibited 7,12-dimethylbenz[a]anthracene-induced tumorigenesis possibly by effects of TCDD exerted during the initial exposure period to 12-dimethylbenz[a]anthracene.

In summary, the present study shows that the liver of three strains of female mice that have the same AhR^{b2} genotype, respond differently to TCDD with respect to the number of genes that are up- and down-regulated 24 h after exposure. In particular the GSTm-class of genes were markedly induced by TCDD but only in BALB mice. These findings are of interest inasmuch as expression of GST family genes, in particular *GSTm*, reflect a distinct susceptibility to carcinogenicity by polycyclic aromatic hydrocarbons. The modulating biomolecules that transactivate *GSTm* genes and modify the carcinogenic susceptibility to PAHs may exist in BALB mice. The present experimental model using BALB and CBA strains having an identical AhR^{b2} genotype may be useful for ultimately identifying those genes that might be responsible for strain differences in susceptibility to chemical-induced toxicity and carcinogenicity.

Acknowledgements—The authors thank Dr Hiromi Sato, Institute of Medical Molecular Design, Inc., and Dr Shigeyuki Uno, Nihon University School of Medicine, for their technical suggestions regarding the detection of B[a]P-induced DNA adducts. This work was supported in part by grants from the Environmental Technology Development Fund (S.O.) and Environmental Risk Office Fund (C.T.) of the Ministry of the Environment, Japan.

References

Bartsch H. 2000. Studies on biomarkers in cancer etiology and prevention: a summary and challenge of 20 years of interdisciplinary research. *Mutat. Res.* **462**: 255–279.

Chapman DE, Schiller CM. 1985. Dose-related effects of 2,3,7,8-tetrachlorodibenzo-*p*-dioxin (TCDD) in C57BL/6J and DBA/2J mice. *Toxicol. Appl. Pharmacol.* **78**: 147–157.

Dinkova-Kostova AT, Holtzclaw WD, Cole RN, Itoh K, Wakabayashi N, Katoh Y, Yamamoto M, Talalay P. 2002. Direct evidence that sulfhydryl groups of Keap1 are the sensors regulating induction of phase 2 enzymes that protect against carcinogens and oxidants. *Proc. Natl Acad. Sci. USA* **99**: 11908–11913.

Ema M, Ohe N, Suzuki M, Mimura J, Sogawa K, Ikawa S, Fujii-Kuriyama Y. 1994. Dioxin binding activities of polymorphic forms of mouse and human arylhydrocarbon receptors. *J. Biol. Chem.* **269**: 27337–27343.

Gelboin HV. 1980. Benzo[alpha]pyrene metabolism, activation and carcinogenesis: role and regulation of mixed-function oxidases and related enzymes. *Physiol Rev.* **60**: 1107–1166.

Gupta RC, Reddy MV, Randerath K. 1982. 32P-postlabeling analysis of non-radioactive aromatic carcinogen — DNA adducts. *Carcinogenesis* **3**: 1081–1092.

Hayes JD, Pulford DJ. 1995. The glutathione S-transferase supergene family: regulation of GST and the contribution of the isoenzymes to cancer chemoprotection and drug resistance. *Crit. Rev. Biochem. Mol. Biol.* **30**: 445–600.

Holcomb M, Safe S. 1994. Inhibition of 7,12-dimethylbenzanthracene-induced rat mammary tumor growth by 2,3,7,8-tetrachlorodibenzo-*p*-dioxin. *Cancer Lett.* **82**: 43–47.

Kawakami T, Ishimura R, Nohara K, Takeda K, Tohyama C, Ohsako S. 2006. Differential susceptibilities of Holtzman and Sprague-Dawley rats to fetal death and placental dysfunction induced by 2,3,7,8-tetrachlorodibenzo-*p*-dioxin (TCDD) despite the identical primary structure of the aryl hydrocarbon receptor. *Toxicol. Appl. Pharmacol.* **212**: 224–236.

Moriguchi T, Motohashi H, Hosoya T, Nakajima O, Takahashi S, Ohsako S, Aoki Y, Nishimura N, Tohyama C, Fujii-Kuriyama Y, Yamamoto M. 2003. Distinct response to dioxin in an arylhydrocarbon receptor (AHR)-humanized mouse. *Proc. Natl Acad. Sci. USA* **100**: 5652–5657.

Ohsako S, Miyabara Y, Sakaue M, Ishimura R, Kakeyama M, Izumi H, Yonemoto J, Tohyama C. 2002. Developmental stage-specific effects of perinatal 2,3,7,8-tetrachlorodibenzo-*p*-dioxin exposure on reproductive organs of male rat offspring. *Toxicol. Sci.* **66**: 283–292.

Pohjanvirta R, Tuomisto J. 1994. Short-term toxicity of 2,3,7,8-tetrachlorodibenzo-*p*-dioxin in laboratory animals: effects, mechanisms, and animal models. *Pharmacol. Rev.* **46**: 483–549.

Pohjanvirta R, Wong JM, Li W, Harper PA, Tuomisto J, Okey AB. 1998. Point mutation in intron sequence causes altered carboxyl-terminal structure in the aryl hydrocarbon receptor of the most 2,3,7,8-tetrachlorodibenzo-*p*-dioxin-resistant rat strain. *Mol. Pharmacol.* **54**: 86–93.

Prochaska HJ, Talalay P. 1988. Regulatory mechanisms of monofunctional and bifunctional anticarcinogenic enzyme inducers in murine liver. *Cancer Res.* **48**: 4776–4782.

Ramos-Gomez M, Kwak MK, Dolan PM, Itoh K, Yamamoto M, Talalay P, Kensler TW. 2001. Sensitivity to carcinogenesis is increased and chemoprotective efficacy of enzyme inducers is lost in nrf2 transcription factor-deficient mice. *Proc. Natl Acad. Sci. USA* **98**: 3410–3415.

Robertson IG, Guthenberg C, Mannervik B, Jernstrom B. 1986. Differences in stereoselectivity and catalytic efficiency of three human glutathione transferases in the conjugation of glutathione with 7 beta,8 alpha-dihydroxy-9 alpha,10 alpha-oxy-7,8,9,10-tetrahydrobenzo(a)pyrene. *Cancer Res.* **46**: 2220–2224.

Robinson SW, Clothier B, Akhtar RA, Yang AL, Latour I, Van Ijperen C, Festing MF, Smith AG. 2002. Non-ahr gene susceptibility loci for porphyria and liver injury induced by the interaction of 'dioxin' with iron overload in mice. *Mol. Pharmacol.* **61**: 674–681.

Sato H, Suzuki KT, Sone H, Yamano Y, Kagawa J, Aoki Y. 2003. DNA-adduct formation in lungs, nasal mucosa, and livers of rats exposed to urban roadside air in Kawasaki City, Japan. *Environ. Res.* **93**: 36–44.

Schecter A, Birnbaum L, Ryan JJ, Constable JD. 2006. Dioxins: an overview. *Environ. Res.* **101**: 419–428.

Shimizu Y, Nakatsuru Y, Ichinose M, Takahashi Y, Kume H, Mimura J, Fujii-Kuriyama Y, Ishikawa T. 2000. Benzo[a]pyrene carcinogenicity is lost in mice lacking the aryl hydrocarbon receptor. *Proc. Natl Acad. Sci. USA* **97**: 779–782.

Sims P, Grover PL, Swaisland A, Pal K, Hewer A. 1974. Metabolic activation of benzo(a)pyrene proceeds by a diol-epoxide. *Nature* **252**: 326–328.

Sundberg K, Widersten M, Seidel A, Mannervik B, Jernstrom B. 1997. Glutathione conjugation of bay- and fjord-region diol epoxides of polycyclic aromatic hydrocarbons by glutathione transferases M1-1 and P1-1. *Chem. Res. Toxicol.* **10**: 1221–1227.

Thomas RS, Penn SG, Holden K, Bradfield CA, Rank DR. 2002. Sequence variation and phylogenetic history of the mouse Ahr gene. *Pharmacogenetics* **12**: 151–163.

Tuomisto JT, Viluksela M, Pohjanvirta R, Tuomisto J. 1999. The AH receptor and a novel gene determine acute toxic responses to TCDD:

DOI: 10.1002/jat

segregation of the resistant alleles to different rat lines. *Toxicol. Appl. Pharmacol.* **155**: 71–81.

Unkila M, Pohjanvirta R, MacDonald E, Tuomisto JT, Tuomisto J. 1994. Dose response and time course of alterations in tryptophan metabolism by 2,3,7,8-tetrachlorodibenzo-*p*-dioxin (TCDD) in the most TCDD-susceptible and the most TCDD-resistant rat strain: relationship with TCDD lethality. *Toxicol. Appl. Pharmacol.* **128**: 280–292.

Uno S, Dalton TP, Derkenne S, Curran CP, Miller ML, Shertzer HG, Nebert DW. 2004. Oral exposure to benzo[a]pyrene in the mouse: detoxication by inducible cytochrome P450 is more important than metabolic activation. *Mol. Pharmacol.* **65**: 1225–1237.

Wakabayashi N, Itoh K, Wakabayashi J, Motohashi H, Noda S, Takahashi S, Imakado S, Kotsuji T, Otsuka F, Roop DR, Harada T, Engel JD, Yamamoto M. 2003. Keap1-null mutation leads to postnatal lethality due to constitutive Nrf2 activation. *Nat. Genet.* **35**: 238–245.

Wu Q, Ohsako S, Ishimura R, Suzuki JS, Tohyama C. 2004. Exposure of mouse preimplantation embryos to 2,3,7,8-tetrachlorodibenzo-*p*-dioxin (TCDD) alters the methylation status of imprinted genes H19 and Igf2. *Biol. Reprod.* **70**: 1790–1797.

DOI: 10.1002/jat

特集　子どもと環境化学物質

プログラムされる“病”の新たな仮説

――環境化学物質による代謝系遺伝子の次世代エピゲノム変化

大迫誠一郎 おおさこ　せいいちろう
（東京大学大学院医学系研究科 疾患生命工学センター 健康環境医工学部門）

妊娠中に薬物を服用し，その作用で先天異常（奇形）が起きるという事例は多い．しかし，目に見える異常ではないものの，胎児や新生児などの感受性の高い時期に生じた体の中の変化（素因）が成熟してからも残り，病気へのかかりやすさを決めているのではないかという問題が最近注目され始めている．ダイオキシンのように環境中の極微量の化学物質は，日常生活レベルでは重篤な影響を与えないが，私たちの体の中に目に見えないなんらかの変化を起こしているようだ．この稿ではエピジェネティクスの観点から，そのメカニズムに関して考えてみたい．

バーカー仮説とエピジェネティクス

英国の疫学者 Barker は，イギリスで心臓病の多発する地域には貧しい地域が多かったことから，小児期，新生児期，さらに胎児期までさかのぼって原因を追究した．その結果，低出生体重児（2500 g 未満）で生まれた児は，成人になってから心血管障害発症，肥満，耐糖能異常，高血圧などいわゆるメタボリックシンドローム発症の高リスク群であるという統計学的結果が出た．どうやら，母親が妊娠中に低栄養であって生まれた児は，将来生活習慣病にかかりやすいらしい．この Barker 仮説は一見突拍子もない説に見えたが，これを裏付ける研究結果が続き，近年この概念は，Developmental Origins of Health and Disease（DOHaD）説なるものに発展している[1]．これは「次世代の健康および疾患の素因は，受精卵環境，胎内環境，乳児期環境で決まる」という説である．

DOHaD 説はまだ完全に証明されたわけではないが，その分子生物学的根拠として，「エピジェネティクス」が考えられている．エピジェネティクスは，クロマチンへの後天的な修飾により，遺伝子発現が制御されることに起因する遺伝学・分子生物学の研究分野である．“エピ”とはギリシア語で“後”の意で，DNA 配列以外の修飾（DNA 配列の“後”の修飾）の重要性を示している．DNA のメチル化（塩基のうちシトシンの 5 位がメチル化）やヒストン修飾（アミノ酸残基の主にリジンやアルギニンにアセチル化やメチル化を受ける）などが「エピゲノム」とよばれ情報を制御している．これらエピゲノムのパターンは細胞が分裂しても，娘細胞に受け継がれるため，一種の遺伝情報と見なすことができる．そしてその修飾の度合いは，遺伝子の発現レベルを大きく左右する．

大まかには DNA メチル化は転写を抑制，ヒストンに関してはアセチル化で転写を誘導するとされている．したがってエピゲノム情報の違いは，個体の形質決定にも大きく影響する．そもそも，一つの受精卵から，神経細胞や肝細胞などさまざまな遺伝子発現パターンの異なる細胞が分かれていく（分化する）ことの説明として，DNA 配列以外の機構が想定されていたわけだが，その本体が見えてきたわけだ．ところが近年，その機構が他の生命現象にも及んでいることが見出されてきた．たとえば，ガン細胞はなぜ生じるのかと聞かれると，DNA の配列に変化が起きるから，というのがこれまでの常套句だったわけだが，DNA の高メチル化も原因となる．これはエピジェネティック発ガンと呼ばれている．そして，胎児環境の影

響がDNAメチル化やヒストン修飾に変化を与え，それが生後まで残ることで，各種の遺伝子の発現調節機構が変化することも実験的に確かめられてきた[2]．

胎児期ダイオキシン曝露と発ガンリスクの上昇

DOHaDを左右する環境要因はBarker仮説に見られるような栄養状態だけではなく，化学物質の曝露も対象となる．それを，易発ガン体質(ガンになりやすさ)という事例で下記に示したい．ベンゾ[a]ピレン(BaP)やジメチルベンゾアントラセン(DMBA)といった多環芳香族炭化水素は，たばこのタールの中に含まれる化学物質で，これら物質が原因となってDNAに変異が起こり，ガンが発生することは古くから知られている．100年前，東京帝国大学医学部の山際勝三郎博士がウサギの耳にコールタールを塗りつけて世界で初めて人工的にガンを作ることに成功したが，そのときの原因物質がこれら多環芳香族炭化水素であった．これら化合物は遺伝子に変異を起こす化学物質ということで，変異原物質(mutagen)と呼ばれる．変異原物質はその細胞内受容体分子としてアリール炭化水素受容体(AhR)に結合し，標的遺伝子であるチトクロムP450(CYP)ファミリーの1A1や1B1といった薬物代謝第1相酵素遺伝子(CYPファミリー遺伝子)の転写誘導を起こす．CYPファミリーは，自身を誘導させた変異原物質を酸化反応により化学変化させ，通常は第2相酵素である抱合化酵素に受け渡して体外排出させる．CYPファミリーはいわば生体防御システムの主役の一つである．しかし，変異原物質の酸化反応により生じるBaPエポキシドやDMBAエポキシドのようなエポキシ体はDNA中のグアニン残基へ共有結合してしまうため，DNA配列に変異を起こしうる(これを変異原物質の代謝活性化という)．これが原因となって発ガンへと至るわけである(図1)．

2,3,7,8-四塩素化ジベンゾ-*p*-ジオキシン(TCDD)はダイオキシン類のなかで最も毒性が強く，残留性の高い環境汚染物質である．TCDDの標的である細胞内受容体分子はBaPやDMBAと同じAhRである．しかし，TCDDは環境中でも生体内でも安定すぎる化学物質であるため，変異原物質とは異なりDNAに直接に化学反応を起こすことはない．すなわちダイオキシン自体に発ガン性はない．ところが，胎児期にTCDD曝露されたラットでは，成熟後にDMBAを投与されると，対照群(胎児期にTCDD曝露されていないラット)に比べて乳ガンの発症率が2倍に上昇する[3]．ちなみに，成熟個体に対するTCDDとDMBAの同時投与(複合曝露)では，逆に発ガン率はTCDDによって抑えられる[4]．ダイオキシンに胎児期に曝露された動物がガンにかかりやすくなるという，この感受性逆亢進現象は，他の研究グループでも確認され，筆者も最近行ったマウスを用いた胃ガン誘導実験で同様の結果を得ている(図2)．このようにして生まれてきた動物では，興味深いことにBaPやDMBAの成熟後の曝露，

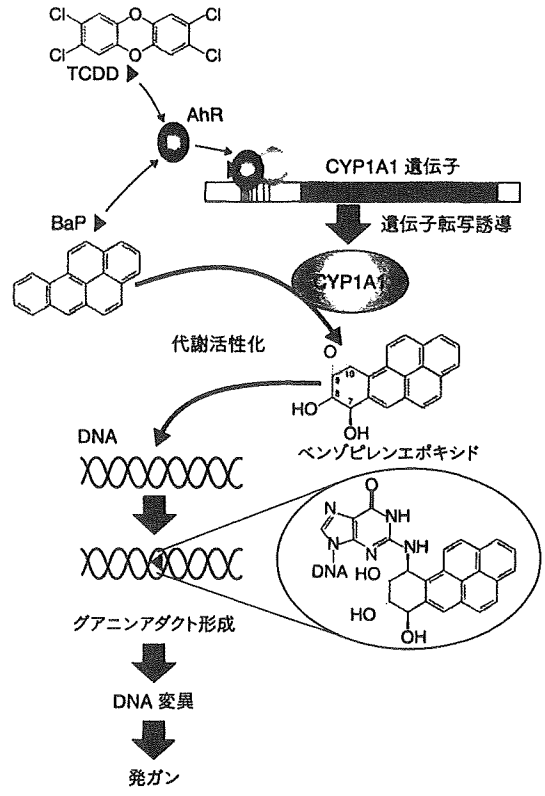

図1——変異原物質ならびにダイオキシンによるCYP遺伝子の誘導と代謝活性化による変異原物質のDNAへの結合．

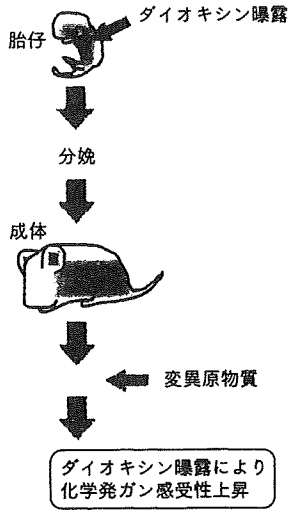

図2——胎児期ダイオキシン曝露で生まれた動物はガンに罹りやすくなる.

あるいはTCDDの再曝露で，肝臓内CYPファミリーの誘導率が，対照群に比べて数倍も高くなる．肝臓の器官としての性質から薬物代謝酵素の強誘導化現象が起こるわけである[5]．胎児期にダイオキシン曝露された動物が，成熟後の変異原曝露でガンになりやすいのは，このCYPファミリーの転写誘導の異常によって，変異原物質の代謝活性化が高くなってエポキシ体の生成がより多くなり，DNAの変異もより高頻度になるため，化学発ガン感受性が亢進すると解釈ができる．

だが，なぜ胎児期にダイオキシン曝露を受けるとCYPファミリーの誘導能に差が生じるのだろう．

ダイオキシンによるエピゲノム変化とその維持

そこで筆者は，マウス妊娠13日目に体重1 kgあたり3 μgのTCDDまたはコーンオイルを投与し，生まれた雌を120日齢まで飼育した．（ちなみにこのようにして生まれた仔のCYP1A1誘導性は，変異原物質やダイオキシンの再投与で数倍高くなることは確認済み.）これら動物から肝臓

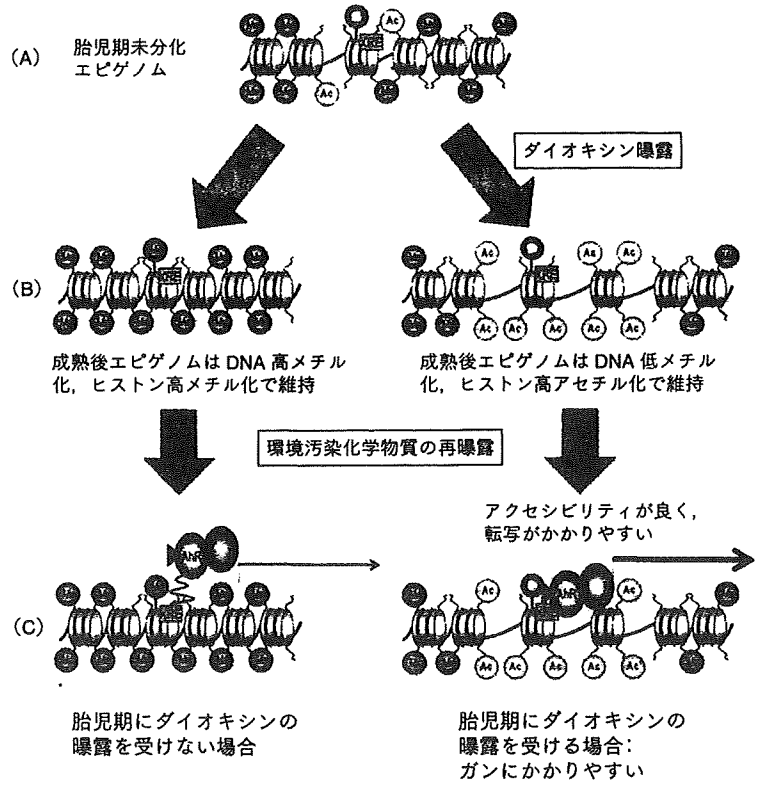

図3——胎児期ダイオキシン曝露によるエピゲノム変化と遺伝子の誘導性の差異を生じさせる機構．(A)胎児期の未分化なエピゲノム構造．(B)胎児期TCDD曝露後，成熟後まで維持されるエピゲノムの差．(C)変異原物質やダイオキシン類の再曝露で誘導性が異なる仮説．化学物質と受容体(AhR)複合体の標的遺伝子へのアクセシビリティ(到達性)の違い．